# WEST Search History

DATE: Monday, March 18, 2002

| Set Name side by side | Query | Hit Count | Set Name result set |
|---|---|---|---|
| | *DB=USPT,JPAB,EPAB,DWPI; PLUR=YES; OP=ADJ* | | |
| L36 | trubniyakov.in. and cell$4 | 0 | L36 |
| L35 | schiffenbauer.in. and cell$4 | 3 | L35 |
| L34 | schiffenbauer.in. | 5 | L34 |
| L33 | chaitchik.in. | 3 | L33 |
| L32 | L31 and l2 | 1 | L32 |
| L31 | l15 and (proteol$5 and trypsin) | 47 | L31 |
| L30 | L1 and (fluorescence adj3 (intensit$3 or polarization)) | 31 | L30 |
| L29 | L28 and (fluorescence adj3 (intensit$3 or polarization)) | 0 | L29 |
| L28 | l1 and l2 | 29 | L28 |
| L27 | L26 and (sensitiv$1 adj5 (drug$1 or compound$1 or toxi$4 or chemotherap$5)) | 1 | L27 |
| L26 | L22 and cytomet$3 | 11 | L26 |
| L25 | L22 and l2 | 0 | L25 |
| L24 | L22 and l1 | 0 | L24 |
| L23 | L22 and l1 and l2 | 0 | L23 |
| L22 | L21 same (fluorescence adj3 (intensit$3 or polarization)) | 31 | L22 |
| L21 | cell$4 same (array$1 or microarray$1) | 68670 | L21 |
| L20 | l1 same (array$1 or microarray$1) | 2 | L20 |
| L19 | L18 and cytomet$3 | 0 | L19 |
| L18 | L15 and l2 | 5 | L18 |
| L17 | L16 and l2 | 0 | L17 |
| L16 | L15 and cytomet$3 | 35 | L16 |
| L15 | l1 and (cultur$3 same harvest$3) | 177 | L15 |
| L14 | l1 near50 (cultur$3 same harvest$3) | 0 | L14 |
| L13 | L11 and cytomet$3 | 2 | L13 |
| L12 | L11 and cytomet$1 | 0 | L12 |
| L11 | l2 and l7 | 17 | L11 |
| L10 | L9 and cytomet$3 | 5 | L10 |
| L9 | l7 and l1 | 61 | L9 |
| L8 | L7 and l4 | 5 | L8 |
| L7 | (drug$1 or compound$1 or toxi$4 or chemotherap$5) adj5 (encapsulat$3 or micelle$1 or virus or liposome$1) | 12743 | L7 |
| L6 | l2 and l4 | 5 | L6 |
| L5 | l1 near50 cytomet$3 | 3 | L5 |
| L4 | L1 and cytomet$3 | 107 | L4 |

| | | | |
|---|---|---|---|
| L3 | cytomet$3 near5 (sensitiv$1 adj5 (drug$1 or compound$1 or toxi$4 or chemotherap$5)) | 0 | L3 |
| L2 | (test$3 or detect$3 or determin$5 or evaluat$3 or assay$3) adj3 (sensitiv$1 adj5 (drug$1 or compound$1 or toxi$4 or chemotherap$5)) | 240 | L2 |
| L1 | cell$4 near5 (sensitiv$1 adj5 (drug$1 or compound$1 or toxi$4 or chemotherap$5)) | 784 | L1 |

END OF SEARCH HISTORY

WEST

**End of Result Set**

Generate Collection | Print

L5: Entry 3 of 3 File: DWPI Dec 28, 2000

DERWENT-ACC-NO: 2001-102716
DERWENT-WEEK: 200111


TITLE: Inhibiting plasma membrane uncoupling protein expression in tumor cells and rapidly dividing bacterial cells, for treating cancer and infectious diseases

INVENTOR: NEWELL, M K

PATENT-ASSIGNEE: UNIV VERMONT & STATE AGRIC COLLEGE (UYVEN)

PRIORITY-DATA: 1999US-140574P (June 23, 1999)

PATENT-FAMILY:

| PUB-NO | PUB-DATE | LANGUAGE | PAGES | MAIN-IPC |
|---|---|---|---|---|
| WO 200078941 A2 | December 28, 2000 | E | 106 | C12N015/00 |
| AU 200057600 A | January 9, 2001 | | 000 | C12N015/00 |

DESIGNATED-STATES: AE AG AL AM AT AU AZ BA BB BG BR BY BZ CA CH CN CR CU CZ DE DK DM DZ EE ES FI GB GD GE GH GM HR HU ID IL IN IS JP KE KG KP KR KZ LC LK LR LS LT LU LV MA MD MG MK MN MW MX MZ NO NZ PL PT RO RU SD SE SG SI SK SL TJ TM TR TT TZ UA UG UZ VN YU ZA ZW AT BE CH CY DE DK EA ES FI FR GB GH GM GR IE IT KE LS LU MC MW MZ NL OA PT SD SE SL SZ TZ UG ZW

APPLICATION-DATA:

| PUB-NO | APPL-DATE | APPL-NO | DESCRIPTOR |
|---|---|---|---|
| WO 200078941A2 | June 22, 2000 | 2000WO-US17245 | |
| AU 200057600A | June 22, 2000 | 2000AU-0057600 | |
| AU 200057600A | | WO 200078941 | Based on |

INT-CL (IPC): C12 N 15/00

ABSTRACTED-PUB-NO: WO 200078941A
BASIC-ABSTRACT:

NOVELTY - Inhibiting plasma membrane uncoupling protein (UCP) expression in a cell, comprising contacting a cell with a plasma membrane UCP inhibitor (I), is new.

DETAILED DESCRIPTION - INDEPENDENT CLAIMS are also included for the following:

(1) a composition (II) comprising a plasma membrane targeted UCP inhibitor;

(2) sensitizing (III) a resistant tumor cell to a cytotoxic therapy, by expressing a functional UCP or UCP fragment in a plasma membrane of a resistant tumor cell to sensitize the resistant tumor cell to a cytotoxic therapy;

(3) screening (IV) a tumor cell of a subject for susceptibility to treatment with a chemotherapeutic agent, or screening a subject for the presence of rapidly dividing cells, comprising:

(a) isolating a tumor cell or sample of cells from the subject; and

(b) detecting the presence of a UCP molecule in the plasma membrane of the cell, where the presence of UCP molecule indicates that the tumor cell is susceptible to treatment with a chemotherapeutic agent and is a rapidly dividing cell;

(4) a kit (V) for screening a tumor cell of a subject for susceptibility to treatment with a chemotherapeutic agent, comprising a container housing a UCP molecule detection reagent and instructions for using the reagent;

(5) inducing (VI) cellular division in a growth arrested cell, by expressing a functional UCP or UCP fragment in a plasma membrane of a growth arrested cell to induce cell division of the cell;

(6) regulating (VII) lysosomal pH, by modifying lysosomal UCP activity in a cell;

(7) treating (VIII) autoimmune disease, by administering a UCP activator to a subject to prevent antigen presentation; and

(8) a composition (IX) comprising a UCP inhibitor associated with a lysosomal targeting molecule or a UCP associated with a plasma membrane targeting molecule; and

(9) treating or preventing (X) an infectious disease by administering a lysosomal UCP inhibitor to a subject having or at risk of developing an infectious disease.

ACTIVITY - Antibacterial; antiviral; antifungal; cytostatic; immunosuppressive; antirheumatic; antiarthritic; dermatological.

The effect of UCP inhibitor to cause cell death was studied. Chemotherapy-sensitive cells HL60 and chemotherapy resistant cells HL60-MDR were exposed to a labeled anti-UCP antibody for two 15 minute intervals and subjected to flow cytometry. When HL60s were treated with the anti-UCP antibody, a high number of dead cells were present in the population and longer incubation times with the anti-UCP antibody resulted in a greater number of dead cells within the population. There was no difference between the anti-UCP untreated and treated HL60-MDR cells as these cells do not express cell surface UCP.

MECHANISM OF ACTION - UCP inhibitor.

USE - The method is useful for inhibiting plasma membrane UCP expression in a tumor cell, lymphocyte, pancreatic beta cell, rapidly dividing bacterial cell or B cell. (II) is useful for preventing or treating cancer. (III) is useful for sensitizing a melanoma cell to a cytotoxic therapy. (VI) is useful for inducing cellular division in a nerve cell. (X) is useful for preventing or treating an infectious disease in a subject infected with an intracellular bacteria or parasite. (All claimed). Inhibiting plasma UCP expression in a cell is also useful for treating other diseases associated with rapidly dividing cells such as rheumatoid arthritis and scleroderma.

ABSTRACTED-PUB-NO: WO 200078941A
EQUIVALENT-ABSTRACTS:

CHOSEN-DRAWING: Dwg.0/0

DERWENT-CLASS: B04 D16
CPI-CODES: B04-C01; B04-E02F; B04-F0100E; B04-G01; B11-C08; B12-K04A; B12-K04F; B14-A01; B14-A02; B14-A04; B14-B02; B14-C06; B14-C09B; B14-H01; D05-C12; D05-H09; D05-H12A; D05-H14B2; D05-H16A; D05-H17A6;

# WEST Search History

DATE: Monday, March 18, 2002

| Set Name side by side | Query | Hit Count | Set Name result set |
|---|---|---|---|
| | *DB=USPT,JPAB,EPAB,DWPI; PLUR=YES; OP=ADJ* | | |
| L36 | trubniyakov.in. and cell$4 | 0 | L36 |
| L35 | schiffenbauer.in. and cell$4 | 3 | L35 |
| L34 | schiffenbauer.in. | 5 | L34 |
| L33 | chaitchik.in. | 3 | L33 |
| L32 | L31 and l2 | 1 | L32 |
| L31 | l15 and (proteol$5 and trypsin) | 47 | L31 |
| L30 | L1 and (fluorescence adj3 (intensit$3 or polarization)) | 31 | L30 |
| L29 | L28 and (fluorescence adj3 (intensit$3 or polarization)) | 0 | L29 |
| L28 | l1 and l2 | 29 | L28 |
| L27 | L26 and (sensitiv$1 adj5 (drug$1 or compound$1 or toxi$4 or chemotherap$5)) | 1 | L27 |
| L26 | L22 and cytomet$3 | 11 | L26 |
| L25 | L22 and l2 | 0 | L25 |
| L24 | L22 and l1 | 0 | L24 |
| L23 | L22 and l1 and l2 | 0 | L23 |
| L22 | L21 same (fluorescence adj3 (intensit$3 or polarization)) | 31 | L22 |
| L21 | cell$4 same (array$1 or microarray$1) | 68670 | L21 |
| L20 | l1 same (array$1 or microarray$1) | 2 | L20 |
| L19 | L18 and cytomet$3 | 0 | L19 |
| L18 | L15 and l2 | 5 | L18 |
| L17 | L16 and l2 | 0 | L17 |
| L16 | L15 and cytomet$3 | 35 | L16 |
| L15 | l1 and (cultur$3 same harvest$3) | 177 | L15 |
| L14 | l1 near50 (cultur$3 same harvest$3) | 0 | L14 |
| L13 | L11 and cytomet$3 | 2 | L13 |
| L12 | L11 and cytomet$1 | 0 | L12 |
| L11 | l2 and l7 | 17 | L11 |
| L10 | L9 and cytomet$3 | 5 | L10 |
| L9 | l7 and l1 | 61 | L9 |
| L8 | L7 and l4 | 5 | L8 |
| L7 | (drug$1 or compound$1 or toxi$4 or chemotherap$5) adj5 (encapsulat$3 or micelle$1 or virus or liposome$1) | 12743 | L7 |
| L6 | l2 and l4 | 5 | L6 |
| L5 | l1 near50 cytomet$3 | 3 | L5 |
| L4 | L1 and cytomet$3 | 107 | L4 |

| | | | |
|---|---|---|---|
| L3 | cytomet$3 near5 (sensitiv$1 adj5 (drug$1 or compound$1 or toxi$4 or chemotherap$5)) | 0 | L3 |
| L2 | (test$3 or detect$3 or determin$5 or evaluat$3 or assay$3) adj3 (sensitiv$1 adj5 (drug$1 or compound$1 or toxi$4 or chemotherap$5)) | 240 | L2 |
| L1 | cell$4 near5 (sensitiv$1 adj5 (drug$1 or compound$1 or toxi$4 or chemotherap$5)) | 784 | L1 |

END OF SEARCH HISTORY

## Gabel, Gailene

**To:** STIC-ILL
**Subject:** 09/752,453

Please provide a copy of the following literature:

1) Gaudray et al "Fluorescent Methotrexate Labeling and Flow-Cytometric Analysis . . . " J. Biol. Chem. 261:6285-6292 (May 1986).

2) Morris, G. et al., "Cysteine Proteinase Inhibotors And Bleomycin-Sensitive And -Resistant Cells", Biochemical Pharmacology, vol. 41, No. 11, pp. 1559-1566, 1991.

3) Herweijer et al., A Rapid and Sensitive Flow Cytometric Method for the Detection of Multidrug-Resistant Cells," Cytometry, 10: 463-468,(1989).

Thanks a bunch!!!

Gail Gabel
7B15
CM1
305-0807

**STIC-ILL**

QP501J7

**From:** Gabel, Gailene
**Sent:** Monday, March 18, 2002 12:39 PM
**To:** STIC-ILL
**Subject:** 09/752,453

Please provide a copy of the following literature:

1) Gaudray et al "Fluorescent Methotrexate Labeling and Flow-Cytometric Analysis . . . " J. Biol. Chem. 261:6285-6292 (May 1986).

2) Morris, G. et al., "Cysteine Proteinase Inhibotors And Bleomycin-Sensitive And -Resistant Cells", Biochemical Pharmacology, vol. 41, No. 11, pp. 1559-1566, 1991.

3) Herweijer et al., A Rapid and Sensitive Flow Cytometric Method for the Detection of Multidrug-Resistant Cells," Cytometry, 10: 463-468,(1989).

Thanks a bunch!!!

Gail Gabel
7B15
CM1
305-0807

THE JOURNAL OF BIOLOGICAL CHEMISTRY
© 1986 by The American Society of Biological Chemists, Inc.

Vol. 261, No. 14, Issue of May 15, pp. 6285-6292, 1986
Printed in U.S.A.

# Fluorescent Methotrexate Labeling and Flow Cytometric Analysis of Cells Containing Low Levels of Dihydrofolate Reductase*

(Received for publication, November 27, 1985)

Patrick Gaudray‡, Joseph Trotter, and Geoffrey M. Wahl§

*From the Gene Expression Laboratory, The Salk Institute, San Diego, California 92138*

**Previous studies have demonstrated the usefulness of flow cytometry in the analysis of dihydrofolate reductase (EC 1.5.1.3) gene amplification. However, this powerful and potentially sensitive method for analyzing gene expression in individual cells has not seen widespread use. This is due in part to the difficulty of producing fluorescent methotrexate (Fluo-MTX), which is needed to label dihydrofolate reductase *in vivo*, in yields higher than 1% and of sufficient purity to give low nonspecific backgrounds by the published procedures. We have significantly improved the synthesis of Fluo-MTX to obtain rapidly a chromatographically pure product in 20% yields. In addition, we have found that cell volume is a variable which makes direct comparisons of fluorescence intensity between cell lines difficult. In order to circumvent this problem, we have improved flow cytometric analysis to measure the fluorescence specific intensity of individual cells. A survey of various cells commonly used for gene transfer shows a significant variability in the efficiency with which they are labeled with Fluo-MTX, which appears to be due to variations in their ability to transport this reagent.**



Research over the past decade has demonstrated the importance of gene amplification as a mechanism for generating genomic variability in eukaryotic as well as prokaryotic cells (Schimke, 1982; Stark and Wahl, 1984). In mammals, cytogenetic and molecular evidence of gene amplification is frequently found in tumor cells isolated from cancer patients or grown in tissue culture. Amplification of oncogenes in these cells has led to the hypothesis that their overexpression could be involved in the development and/or progression of malignancy (see Pali, 1981, and Bishop, 1983, for a review). In addition, cell lines established *in vitro*, or tumor cells *in vivo*, can develop resistance to a wide variety of antiproliferative agents through amplification of the gene encoding the enzyme target for the selective drug.

Although gene amplification is a frequent phenomenon in genetic terms ($<10^{-3}$ events/cell/generation), its frequency is too low to allow the molecular analysis of the first events which lead to amplified sequences. Thus, the dynamics of gene amplification have been studied most frequently on large populations of cells which may have undergone numerous genetic changes. One exception has been the study of the amplification of the dihydrofolate reductase gene, which encodes the primary target of the anti-cancer drug methotrexate (MTX[1]) (Hakala *et al.*, 1961). Fluorescent derivatives of MTX (Fluo-MTX; Gapski *et al.*, 1975; Rosowsky *et al.*, 1982) have enabled the labeling of dihydrofolate reductase in individual living cells within a population where it can be quantitated with the flow microfluorometer (FMF) (Kaufman *et al.*, 1978). Furthermore, since the amount of dihydrofolate reductase in a cell is roughly proportional to its dihydrofolate reductase gene copy number (Alt *et al.*, 1978), flow cytofluorometric analysis can give an indication of the dihydrofolate reductase gene copy number per cell under a variety of conditions (Johnston *et al.*, 1983; Mariani and Schimke, 1984).

Our studies have concentrated on the effect of gene position on gene amplification (Wahl *et al.*, 1984). Due to the advantages offered by the analysis of dihydrofolate reductase gene amplification at the level of single cells within a population using the FMF, we have chosen to study the amplification of dihydrofolate reductase minigenes introduced into random genomic locations. It has been necessary to overcome several hurdles in order to pursue these experiments. First, the available dihydrofolate reductase minigenes are usually expressed at low levels in dihydrofolate reductase-deficient CHO cells. While these cells can be transformed to the wild type phenotype by one or a few dihydrofolate reductase minigenes (Crouse *et al.*, 1983), they usually exhibit 20–50% of the wild type levels of dihydrofolate reductase activity. Detection of such low levels of dihydrofolate reductase using the FMF necessitates the use of highly purified Fluo-MTX, free of all the contaminants which cause either a reduction of the signal (*e.g.* MTX) or an unacceptable background fluorescence which prevents sorting. Second, because of the hydrophobicity and low solubility of the product, it has been difficult to produce highly purified Fluo-MTX in yields greater than 1% by the methods published to date (Gapski *et al.*, 1975; Johnston *et al.*, 1983).

In this communication, we report significant alterations of previously published procedures. The method presented enables the preparation of chromatographically pure Fluo-MTX in 20% yields and in one-third the time required previously. We also show that the cell line most commonly used for dihydrofolate reductase gene transfer (DXB11, Urlaub and

* This work was supported in parts by grants from the National Institutes of Health, the G. Harold and Leila Y. Mathers Charitable Foundation, and the Joseph Alexander Foundation. The costs of publication of this article were defrayed in part by the payment of page charges. This article must therefore be hereby marked "*advertisement*" in accordance with 18 U.S.C. Section 1734 solely to indicate this fact.

‡ Recipient of a long term fellowship from the European Molecular Biology Organization.

§ To whom correspondence and requests for reprints should be addressed.

[1] The abbreviations used are: MTX, methotrexate; CHO, Chinese hamster ovary; DMF, dimethylformamide; $Me_2SO$, dimethyl sulfoxide; FBS, fetal bovine serum; FMF, flow microfluorometer; Fluo-DAP, fluoresceinyl-diaminopentane; Fluo-MTX, fluoresceinyl-diaminopentyl-methotrexate; HPLC, high performance liquid chromatography; Hepes, 4-(2-hydroxyethyl)-1-piperazineethanesulfonic acid; DHFR, dihydrofolate reductase; TAC, time to amplitude conversion.

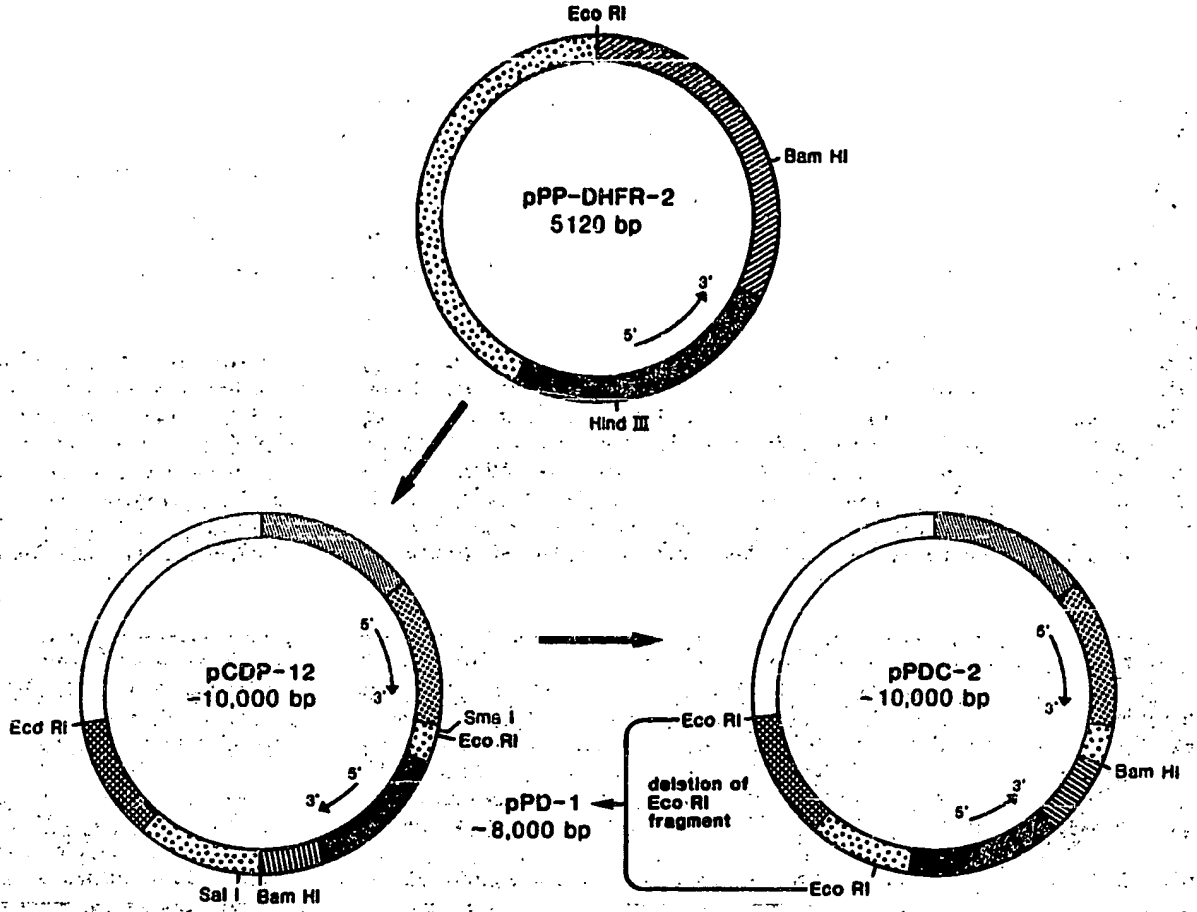


FIG. 1. **Physical and genetic map of dihydrofolate reductase expression vectors.** Sites for restriction enzymes which cut once are indicated. 5'→3' shows the direction of transcription of the *PyrB* and *dihydrofolate reductase* genes. Symbols used are: ▨, pBR322 sequences; □, puc19 sequences; ■, dihydrofolate reductase, and ▩, SV40 sequences derived from pSV2-DHFR (Lee *et al.*, 1981); ▨, mouse mammary tumor virus long terminal repeats sequences from pMDSG (Lee *et al.*, 1981); ▨, *PyrB* gene of *Escherichia coli* coding for the bacterial aspartate transcarbamylase[2]; ■, *Bst*EII/*Eco*RI restriction fragment from cosmid pcos2EMBL (Poustka *et al.*, 1984) carrying the *Cos* site of phage λ; ■, *Bcl*I/*Hph*I fragment of polyoma virus carrying the viral origin of DNA replication and the early transcription promoter/enhancer. *Arrows* show the genealogy of these plasmids. *bp*, base pairs.

Chasin, 1980) expresses the donated genes at the expected levels (10–50% of the wild type dihydrofolate reductase activity) when transformed by different dihydrofolate reductase minigenes, but does not generate wild type transformants which can be labeled with Fluo-MTX at a significant level. Our data suggest that the inability to label DXB11 transformants with Fluo-MTX is due to an impaired transport of Fluo-MTX. On the contrary, dihydrofolate reductase-deficient DG44 cells are well suited for analyzing expression and amplification of donated dihydrofolate reductase genes using Fluo-MTX and flow cytometry. We have also analyzed a variety of cell lines commonly used for gene transfer by flow cytometry after labeling with Fluo-MTX and have found that they differ significantly in their ability to be labeled with Fluo-MTX. The implications of this result are discussed.

## MATERIALS AND METHODS

*Chemicals*—$Me_2SO$ was purchased from Mallinkrodt; DEAE-Trisacryl from LKB; HPLC water and acetonitrile from Baker; NADPH from Boehringer; methotrexate was provided by the National Cancer Institute; and all other chemicals were purchased from Sigma.

*Cells*—Two different dihydrofolate reductase-deficient CHO cells were generously provided by Dr. L. Chasin, Columbia University. DXB11 is a homozygous mutant of CHO-K1 obtained by x-ray mutagenesis (Urlaub and Chasin, 1980). DG44 is a CHO-pro3 cell line containing a double deletion of the dihydrofolate reductase locus, analogous to the other DG cell lines described in Urlaub *et al.* (1983). Mutant as well as wild type CHO-K1 were routinely grown in F12 medium supplemented with 10% FBS. Human and mouse lymphocytes were grown in RPMI medium containing 10% FBS. All other cell lines were grown in Dulbecco's modified Eagle's medium supplemented with 10% FBS.

*Transformation of Dihydrofolate Reductase-deficient Cells*—A modification of the procedure of Shen *et al.* (1982) was used. For transformation of $10^6$ cells, 10 μg of plasmid DNA in 850 μl of sterile water were mixed with 100 μl of 10 × HEBS (10 × HEBS contains 1.37 M NaCl, 50 mM KCl, 7.3 mM $Na_2HPO_4$, 210 mM Hepes/NaOH, and 1% glucose at pH 7.20) in a 15-ml conical clear centrifuge tube. Fifty μl of 2 M $CaCl_2$ were added on the side of the tube and then mixed thoroughly by vortexing for 15 s. After 15 min at room temperature, the mixture was used for transformation. Trypsinized cells, suspended in medium containing 10% FBS, were counted, and aliquots of $10^6$ cells were centrifuged in tubes containing 10 ml of serum-free medium. All but approximately 0.1 ml of supernatant was removed. Cells were resuspended in the remaining medium. The DNA/$Ca^{2+}PO_4$ suspension was added and incubated at 37 °C with occasional gentle agitation for 20–30 min, and then $10^5$–$10^6$ cells were plated in 10-cm dishes in nonselective medium. Medium was changed after 6–18 h at 37 °C, and selection was applied approximately 48 h after the cells were plated. Selective medium was Dulbecco's modified Eagle's me-

[2] J. Ruiz and G. M. Wahl, manuscript in preparation.

dium supplemented with nonessential amino acids and 10% dialyzed FBS. Routinely, $10^{-4}$ to $10^{-3}$ of the cells were transformed to the wild type phenotype.

*Dihydrofolate Reductase Minigene Plasmids*—The structure of the pSV2-DHFR plasmid has been described (Lee *et al.*, 1981). The core module (*Hin*dIII/*Bam*HI fragment) containing the mouse dihydrofolate reductase cDNA, the small-T intron, and early mRNA polyadenylation signal, was introduced into four different expression vectors. These vectors have been constructed for other purposes and thus the detail of their construction is not relevant to the present study. However, their maps are presented in Fig. 1 for interested readers who can obtain further details concerning their construction and properties from the authors.

*Dihydrofolate Reductase Enzyme Activity*—A suspension of $10^7$ cells/ml in 20 mM Tris, pH 8, 0.5 M NaCl, 2 mM dithiothreitol, and 2 mM phenylmethylsulfonyl fluoride was lysed by 8 rounds of freeze-thawing. The lysate was centrifuged for 15 min at 11,000 × *g*. The supernatant was recovered, and protein concentration was determined by the Bio-Rad protein assay (Bradford, 1976). Dihydrofolate reductase enzymatic activity was determined according to Frearson *et al.* (1966). The amount of enzyme needed to convert 1 nmol of dihydrofolate into tetrahydrofolate in 1 min at 25 °C is defined as 1 unit.

*HPLC Analysis*—The stationary phase was a preparative Altex Ultrasphere ODS column (inside diameter: 10 mm × 25 cm; 5-μm diameter particles) and the mobile phase was a gradient mixture of 0.1 M ammonium acetate pH 7.00 (A) and 80% (v/v) acetonitrile, 0.02 M ammonium acetate, pH 7.00 (B). Usually, 10 μl of 1 mM solutions of methotrexate, fluoresceinyl diaminopentane, or Fluo-MTX (made in 90% A + 10% B buffer) were injected for one analysis. The flow rate was 2 ml/min. The absorbance at 254 nm was recorded.

*Flow Cytometry*—Cells at approximately 75% confluency were incubated 18–24 h at 37 °C in F12 medium containing 10% FBS and the indicated concentrations of Fluo-MTX. For each analysis, a negative control was included in which each cell line was labeled in the same conditions, but in the presence of 10–20 μM nonlabeled MTX as a competitor. The excess label was removed by incubation of the cells in drug-free Dulbecco's modified Eagle's medium containing 10% FBS for 30 min at 37 °C before harvesting. A suspension of approximately $10^6$ cells/ml was made in ($Ca^{2+}$ and $Mg^{2+}$)-free phosphate-buffered saline containing 2.5% filtered dialyzed FBS. Flow cytometric data were collected on the Salk Institute FMF via a modified LACEL model 317 data acquisition hardware by a DEC PDP-11/73 computer and stored as listmode data files for subsequent analysis. The FMF multiparameter set-up was as follows: analog signals from the fluorescein channel (515–540 nm) were integrated and logarithmically compressed over a 3-decade range as a measure of total intracellular fluorescence. Forward narrow angle light scatter signals were both integrated as a measure of total scatter and patched to a pulse shape analyzer for time to amplitude conversion (TAC) as a measure of cell diameter. The instrumental gains were set such that autofluorescence from unlabeled cells was on scale when excited at 600 milliwatts by the argon laser tuned to 488 nm. Fluorescence and TAC units represent the geometric means of fluorescence and TAC distributions. The signal-to-noise ratio (S.N.R.) for cells labeled with Fluo-MTX is the difference between the mean fluorescence of the cells labeled with Fluo-MTX alone (*A*) and the mean fluorescence of cells labeled with Fluo-MTX plus free MTX (*B*) (*i.e.* nonspecific fluorescence), divided by the mean fluorescence of cells labeled with Fluo-MTX plus free MTX (S.N.R. = $(A - B)/B$).

*Fluoresceinyl-diaminopentane (Fluo-DAP)*—The synthesis and purification of Fluo-DAP was performed according to Gapski *et al.* (1975). Starting from 1–3 g of fluorescein isothiocyanate, yields of 40% were achieved routinely.

*Fluoresceinyl-diaminopentyl-methotrexate (Fluo-MTX)*—The modifications we have introduced in the synthesis and purification procedure of Gapski *et al.* (1975) are outlined and discussed in detail under "Results." However, a complete protocol is presented here for convenience.

MTX (115 mg) (~$2.5 \times 10^{-4}$ mol), 125 mg of Fluo-DAP (~$2.5 \times 10^{-4}$ mol), and 230 mg of 1-ethyl-3-(3-dimethylaminopropyl)carbodiimide were dissolved in 20 ml of dimethylformamide with magnetic stirring and reacted in the dark for 15 min at room temperature in a 150-ml Corex tube. Diethyl ether (150 ml) was added to stop the reaction. The suspension was centrifuged for 15 min at 3000 rpm. The cloudy supernatant was discarded, and the pellet was air-dried. The pellet was then dissolved in 100 ml of 0.1 M $NH_4OH$ (15 min at room temperature with magnetic stirring) and the solution was clarified by filtration through a 0.45-μm nitrocellulose filter. The solution was brought to pH 6.5–7.0 with 5 N HCl and a precipitate of Fluo-MTX was allowed to form for 5–10 min at room temperature. The precipitate was collected by filtration as before, dried on the filter in a lyophilizer, and then dissolved in 25 ml of 50 mM $NH_4OH$. The clear solution was loaded on a 25-ml DEAE-Trisacryl column, which had previously been extensively washed and equilibrated with $H_2O$. The column was washed overnight with 0.5–1 liter of 0.1 M $NH_4HCO_3$, 20% $CH_3CN$, then with 100 ml of 0.25 M $NH_4CO_3$, 20% $CH_3CN$. A broad peak of fluorescent material was then eluted from the column in 0.5 M $NH_4CO_3$, 20% $CH_3CN$ and collected. The eluted material was homogeneous and co-migrated with Fluo-MTX in thin layer chromatography on polyethyleneimine-cellulose TLC plates using 0.25 M $NH_4HCO_3$, 20% $CH_3CN$ as a solvent ($R_f$ values: MTX = 0.56, Fluo-DAP = 0.36, Fluo-MTX = 0.27). The eluate was brought to pH 3 by addition of 5 N HCl, and the precipitate was collected and dried as before. The brown solid obtained was subsequently dissolved in 20 ml of 50 mM $NH_4OH$ and lyophilized. Alternative methods for storage are described under "Results."

## RESULTS

*Synthesis and Characterization of Fluo-MTX*—We have found that the synthesis of Fluo-MTX by published procedures (Gapski *et al.*, 1975) is compromised by secondary reactions which lead to the accumulation of products that are almost totally insoluble in the commonly used solvents. These reactions are favored by trace amounts of water in the reaction mixture and they dramatically increase with time. This first problem can be minimized by using anhydrous solvents. We have also investigated the kinetics of the reaction in several different solvents in order to optimize the production of Fluo-MTX.[3] Analysis by HPLC of the reaction products generated either in $Me_2SO$ or DMF showed that insoluble products accumulated at the same rate in both solvents. However, the rate of synthesis of Fluo-MTX was significantly greater in DMF than in $Me_2SO$. In DMF, after only a 5-min reaction, more than 40% of the material absorbing at 254 nm was Fluo-MTX, and, after 15–20 min, virtually all free MTX had been converted to fluoresceinated derivatives of MTX. On the contrary, more than 60 min were needed to achieve the same result in $Me_2SO$. Moreover, a rapid purification of Fluo-MTX can be achieved when Fluo-MTX is synthesized in DMF. This purification takes advantage of the miscibility of DMF in diethyl ether and the insolubility of Fluo-MTX in this solvent. Thus, it is possible to stop the reaction efficiently by precipitation of the products with diethyl ether. This procedure cannot be applied to the reaction performed in $Me_2SO$ since $Me_2SO$ is not miscible with diethyl ether.

Fluo-MTX prepared as described above is suitable for cell labeling after an additional acid precipitation. However, the stability of Fluo-MTX after acid precipitation is poor as indicated by the accumulation of insoluble material within a few weeks of storage as a solid at −20 °C. As a consequence, the signal-to-noise ratio (see "Materials and Methods") observed in the analysis of CHO-K1 cells by flow cytofluorometry, drops from >2.5 (with CHO-K1 cells) for fresh product to less than 0.6 within 38 weeks of storage.

In order to obtain a product which is stable upon storage and gives a high signal-to-noise ratio, it is necessary to purify Fluo-MTX further by ion exchange chromatography. This step is problematic using published protocols because Fluo-MTX is hydrophobic and binds to many column matrices. We have used DEAE-Trisacryl in order to limit the nonspecific interaction which is commonly observed in the chromatography of fluorescein derivatives on cellulose columns. We have found that the addition of 20% acetonitrile to buffers

[3] Data not shown.

used to wash and elute Fluo-MTX from the column further helps to reduce the hydrophobic interactions which result in broad peaks and a substantial loss of product.

When purified as described above, Fluo-MTX can be stored at −20 °C in three alternative ways for at least 6 months without apparent loss of activity, solubility, or alterations which increase the background fluorescence. It may be stored as: 1) a 10 mM solution in 10 mM $NH_4OH$, 2) a 10 mM suspension in 1 mM HCl, or 3) a dry solid. Purified Fluo-MTX has a specific absorbance of $E_{1\%,\,450\ nm} = 55{,}200$, $E_{1\%,\,375\ nm} = 12{,}200$, at pH 13. However, while it was homogenous by TLC, the most worrisome contaminant, free MTX, is difficult to detect by this analysis.[3] We thus performed HPLC and monitored the absorbance at 254 nm, a wavelength capable of detecting all of the reactants and products. Fig. 2*B* shows that no free MTX is detectable in Fluo-MTX prepared by our procedure. Two major product peaks were detected. They represent more than 80% of the material absorbing at 254 nm, and are also present in a pure sample of Fluo-MTX (*panel A*, kindly given to us by J. Whiteley, Scripps Clinic and Research Foundation, La Jolla). It is possible that these two products are the $\alpha$ and $\gamma$ isomers of Fluo-MTX. Synthesis and purification of Fluo-MTX according to the procedure described above are reproducible as long as they are not scaled up to produce gram quantities of Fluo-MTX. In fact, we have observed that the yield decreased when large amounts of Fluo-MTX were prepared.[3] One possible explanation is that it is more difficult to control the timing of the reaction and purification when working with large volumes.

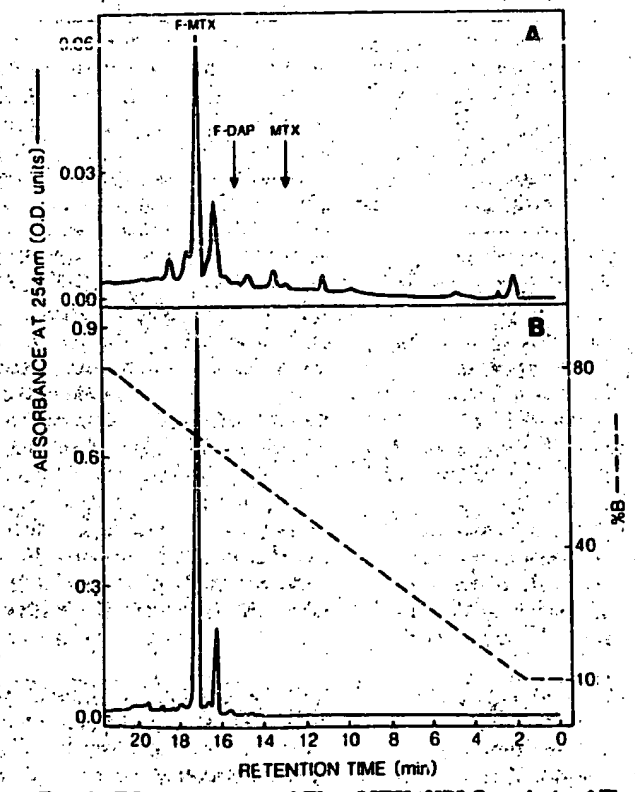


FIG. 2. **HPLC analysis of Fluo-MTX.** HPLC analysis of Fluo-MTX was performed as described under "Materials and Methods." *Panel A* shows the typical pattern of a Fluo-MTX sample provided by Dr. J. Whiteley, as well as the location of Fluo-DAP and MTX peaks run in a parallel experiment. *Panel B* shows the result of the same analysis performed on a Fluo-MTX sample synthesized and purified according to "Materials and Methods."

We assessed the purity of our Fluo-MTX by its ability to inhibit dihydrofolate reductase activity in extracts of CHO-K1 cells. Fig. 3 shows that Fluo-MTX inhibits dihydrofolate reductase strongly although less efficiently than MTX does, as noted by others (Gapski *et al.*, 1975; Kaufman *et al.*, 1978). We have observed that the enzyme encoded by the plasmids pCDP12, pPDC2, and pPD1 (see Fig. 1) in several transformants of DXB11 and DG44 cells shows an altered inhibition by both Fluo-MTX and MTX. One example is shown in Fig. 3 (pCDP-3 cells). Since the dihydrofolate reductase gene present in the plasmid which was used to obtain pCDP-3 transformants was derived from pSV2-DHFR and the latter encodes a kinetically normal enzyme (pSV2-6 in Fig. 3), we infer that the mutation leading to the observed change in MTX binding characteristics must have occurred during cloning.

*Labeling of Cells Expressing Low Levels of Dihydrofolate Reductase with Fluo-MTX*—Previous studies have emphasized the use of Fluo-MTX and flow cytometry to study cells with high levels of dihydrofolate reductase. However, a significant number of experiments require the ability to differentiate accurately among cells expressing low levels of dihydrofolate reductase. Therefore, we have investigated the conditions required to optimize and quantitate the labeling of cells which have low dihydrofolate reductase activity.

Johnston *et al.* (1983) have shown that addition of thymidine, hypoxanthine, and glycine to the labeling medium reverses the toxicity of MTX at least during the time required to attain optimal labeling (≥16 h; Kaufman *et al.*, 1978). We have thus chosen to label cells with Fluo-MTX in F12 medium which contains 3 μM thymidine, 30 μM hypoxanthine, and 100 μM glycine. Under these conditions, less than 1% of the cells labeled overnight with 20 μM Fluo-MTX plus up to 20 μM MTX were dead, as determined by flow cytometry analysis of propidium iodide-labeled cells.

Kaufman *et al.* (1978) have also shown that a relatively high concentration of Fluo-MTX is needed to saturate the enzyme present in a highly amplified line. We have found that 20 μM Fluo-MTX was sufficient to label CHO-C4005 cells, which contain approximately 1,000 dihydrofolate reductase gene copies (Milbrandt *et al.*, 1981; Fig. 4*C*). The intensity of fluorescence in CHOC4005 cells is approximately 500 times higher than in CHO-K1 cells, which is in good agreement with their respective dihydrofolate reductase gene copy numbers (Fig. 4). The distribution of fluorescence in CHOC4005 cells is broader than in CHO-K1 cells. The reason for this has not been investigated in detail, but might be related to a variability in the dihydrofolate reductase gene copy number, which has not been studied previously on a cell by cell basis in this mutant.

The detection and quantitation of cells with low dihydrofolate reductase activity requires that the background fluorescence be minimized. This background results from both the autofluorescence of the cells (*i.e.* fluorescence in the absence of any fluorescein label) and the nonspecific retention of Fluo-MTX within or absorbed to the cells. In order to determine the background fluorescence, we have labeled the cells in 20 μM MTX in addition to Fluo-MTX (Fig. 4, *D*, *E*, and *F*). In the labeling conditions used in Fig. 4 (20 μM Fluo-MTX), the background fluorescence proved to be minimal relative to the signal for the highly amplified CHOC4005 cells (background ≤0.7% of the signal, Fig. 4, *C* and *F*), even though the competing MTX was present only at the same molarity as the Fluo-MTX. This observation confirms that MTX is more efficient than Fluo-MTX in binding dihydrofolate reductase *in vivo*. On the other hand, when cells with low levels of

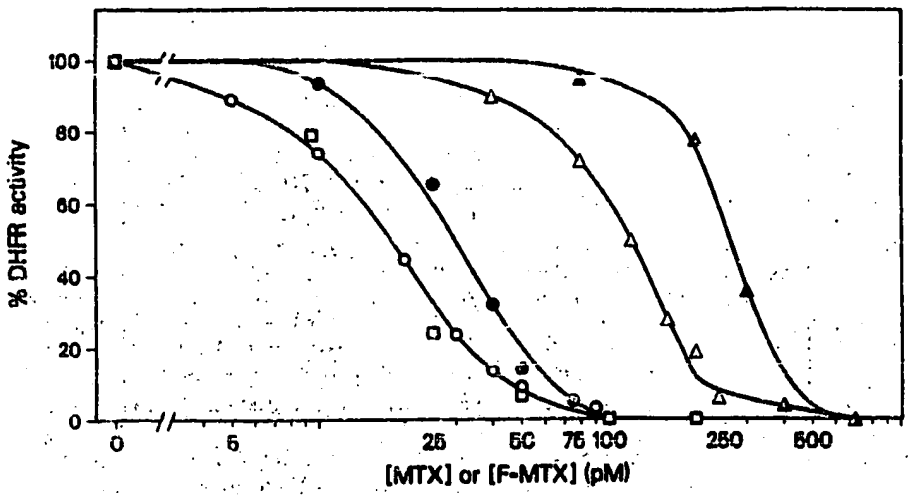


FIG. 3. **Inhibition of dihydrofolate reductase activity by MTX and Fluo-MTX.** Dihydrofolate reductase enzyme (0.3–0.5 milliunits) was assayed spectrophotometrically according to "Materials and Methods." Increasing concentrations of MTX (○, ●, □) or Fluo-MTX (△, ▲) were added in the assay cuvette and initial velocities were determined for each concentration. ○, △, CHO-K1 cell extract; ●, ▲, extract from pCDP3 cells (pCDP-3 is a clone of LXB11 DHFR⁻ cells transformed to DHFR⁺ by transfer of the plasmid pCDP12, see Fig. 1); □, extract from pSV2-6 cells (pSV2-6 is a clone of DG44 DHFR⁻ cells transformed to DHFR⁺ by transfer of the plasmid pSV2-DHFR (Lee *et al.*, 1981)).

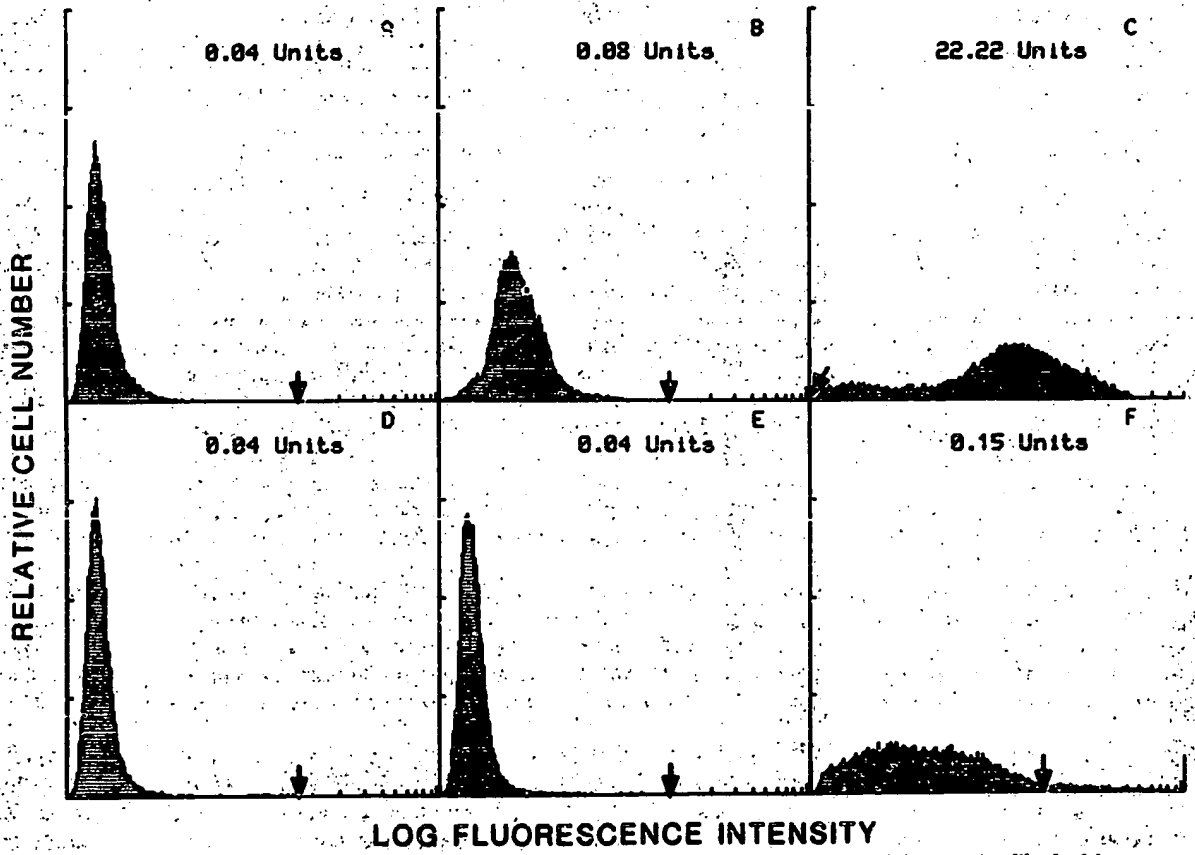


FIG. 4. **Flow cytofluorometric analysis of cells labeled with Fluo-MTX.** DXB-11 (0 dihydrofolate reductase gene/cell; *A* and *D*), CHO-K1 (wild type, ~2 dihydrofolate reductase genes/cell; *B* and *E*), and CHOC4005 (~1000 dihydrofolate reductase genes/cell; *C* and *F*; Milbrandt *et al.*, 1981) cells were labeled for 18 h at 37 °C with either 20 μM Fluo-MTX alone (*A*, *B*, and *C*) or 20 μM Fluo-MTX and 20 μM MTX (*D*, *E*, and *F*), and analyzed according to "Materials and Methods." The *arrow* shows the position of an arbitrary reference channel corresponding therefore to 1 fluorescence unit (*note the change in the scale of panel C*). *Numbers* represent the value for the logarithmic mean of the fluorescence distribution in arbitrary units.

dihydrofolate reductase (*e.g.* CHO-K1 or DG44) were labeled with 20 μM Fluo-MTX, the background was appreciable compared to the signal (background = 50% of the signal, Fig. 4, *A*, *B*, *D*, and *E*). Table I shows that for CHO-K1 cells, the specific signal does not increase between 1 and 20 μM Fluo-MTX, although the background does. Since the background is almost indistinguishable from the autofluorescence of the unlabeled cells when 1 μM Fluo-MTX is used, the maximum signal-to-noise ratio in cells expressing low amounts of dihydrofolate reductase can be achieved by labeling cells at this concentration.

The crude data obtained by flow cytometry (*i.e.* total fluorescence per cell) cannot be directly compared to the dihydrofolate reductase specific enzyme activity which is expressed as a specific activity (*i.e.* dihydrofolate reductase activity per mg of protein). In fact, Kaufman *et al.* (1978) have shown that Fluo-MTX fluorescence is only roughly proportional to dihydrofolate reductase activity among various dihydrofolate reductase amplified cells. In a similar study on nonamplified cells, we have observed the same scattering of experimental points, even in cells transformed with dihydrofolate reductase minigenes which provide a sampling of various low levels of dihydrofolate reductase expressed in the same cellular background (Fig. 5*B*). We have therefore modified our software to normalize the total fluorescence per cell to the relative cell volume. Cell volume was calculated by using TAC as an estimate of cell diameter. The computer algorithm subtracts the $\log_{10}((TAC)^3 \times \text{constant})$ from the $\log_{10}$(total relative fluorescence) for each cell, and generates a new normalized listmode data file. Normalized relative fluorescence per cell volume can be directly compared to the dihydrofolate reductase specific activity as shown in Fig. 5*A*.

The specific dihydrofolate reductase fluorescence of DG44-derived transformants is proportional to their content of dihydrofolate reductase (Fig. 5*A*). The ratio of Fluo-MTX label to dihydrofolate reductase activity does not discriminate among DG44 transformants expressing the wild type dihydrofolate reductase (*e.g.* pSV2-DHFR) or the kinetically altered dihydrofolate reductase described above (encoded by pCDP12 and pPDC2). In these cells, dihydrofolate reductase levels as low as 20% of that in CHO-K1 cells can be detected by flow cytofluorometry. It was surprising that DXB11 transformants show little, if any, signal in the FMF although they contain significant dihydrofolate reductase activity measured in extracts. The unexpectedly low fluorescence level of DXB11 transformants may be related to impaired permeability of Fluo-MTX, since they produce a dihydrofolate reductase enzyme which is efficiently inhibited by Fluo-MTX *in vitro* (Fig. 3). Other cells (*e.g.* FR3T3 and 208-F rat cells, Fig. 5*A*) also seemed to have aberrant ratios of dihydrofolate reductase activity to Fluo-MTX binding suggesting that they too may have an altered permeability to Fluo-MTX. The scattering of the experimental points in Fig. 5*A* shows that the efficiency of the labeling of dihydrofolate reductase with Fluo-MTX varies among different cell lines. Although the specific Fluo-MTX labeling of dihydrofolate reductase in one species appears constant (*e.g.* mouse cells or hamster cell transformants, Fig. 5*A*), exceptions such as W7-TG cells indicate that this observation cannot be generalized.

TABLE I

*Dependence of signal-to-noise ratio on Fluo-MTX concentration*

| Concentration of Fluo-MTX | Total signal (Fluo-MTX alone) (*a*)[a] | Background[b] (Fluo-MTX + MTX) (*b*)[a] | Specific signal (*a* − *b*) | Signal-to-noise ratio (*a* − *b*/*b*) |
|---|---|---|---|---|
| μM | | | | |
| 0 | 1.0[c] | | | |
| 1 | 4.88 | 1.25 | 3.63 | 2.9 |
| 5 | 6.06 | 2.74 | 3.32 | 1.2 |
| 20 | 10.29 | 6.33 | 3.96 | 0.6 |

[a] (*a*) and (*b*) represent the logarithmic mean value of the flow cytometry distribution (see Fig. 4).

[b] Background fluorescence was estimated after labeling cells in the presence of 20 μM MTX at the same time as Fluo-MTX (see "Materials and Methods").

[c] Fluorescence values are given in arbitrary units.

## DISCUSSION

In this communication, we describe a new procedure for preparing Fluo-MTX which should make it easily accessible to laboratories with little or no experience in organic chemistry. High purity Fluo-MTX has been used successfully to label and quantitatively analyze by flow cytometry cells with low dihydrofolate reductase content (~20% of the dihydrofolate reductase specific activity of CHO-K1 cells).

Comparison of Fluo-MTX labeling between different cells—even subclones of the same parental line—can be impaired by the large variability of their volumes. We have therefore created a computer program which allows us to estimate the specific Fluo-MTX fluorescence per volume unit for each cell. We have used this new fluorescence parameter in a comparative survey of different cells commonly used in gene transfer experiments in many laboratories. This analysis reveals that Fluo-MTX labeling efficiency varies between cells. For example, Fisher rat cells are labeled less efficiently than mouse cells. Moreover, different cell lines of the same species also vary in Fluo-MTX labeling efficiency. For example, mouse W7-TG lymphocytes show a reduced Fluo-MTX uptake. However, the close proportionality between fluorescence specific intensity and dihydrofolate reductase specific activity observed within a series of cells derived from the same parental line (DG44 transformants in Fig. 5*A*) shows that flow cytometry is a valuable tool in the study of dihydrofolate reductase gene abundance and expression in cultured cells *in vitro*.

The major progress contributed by flow cytometry in the understanding of gene amplification in cultured cells (Kaufman *et al.*, 1978; Johnston *et al.*, 1983; Mariani and Schimke, 1984) has led to the hope that flow cytometry could also be used for the analysis of clinically relevant forms of methotrexate resistance. However, the variability of the efficiency of the Fluo-MTX labeling among different cells, added to the fact that resistance of cells to MTX can frequently be achieved by means other than dihydrofolate reductase gene amplification (Schimke, 1984), makes it unlikely that flow cytometry can be used with a high degree of certainty to detect the presence of drug resistant cells in tumors isolated from patients. In addition, our observation that the Fluo-MTX concentration used for optimal flow cytometry does not enable discrimination between enzymes which display a 3-fold difference in their affinity for Fluo-MTX suggests that this technique may be relatively insensitive to important enzyme structural changes, some of which could impart clinical drug resistance.

During the course of this work, we have observed that wild type cells, obtained after transformation of dihydrofolate reductase-deficient DXB11 cells by dihydrofolate reductase minigenes, cannot be labeled significantly with Fluo-MTX. However, the enzyme level in these cells is comparable to that of wild type transformants obtained in DG44 cells with the same plasmids. DG44 transformants are easily stained by Fluo-MTX although less efficiently than CHO-K1 cells. This

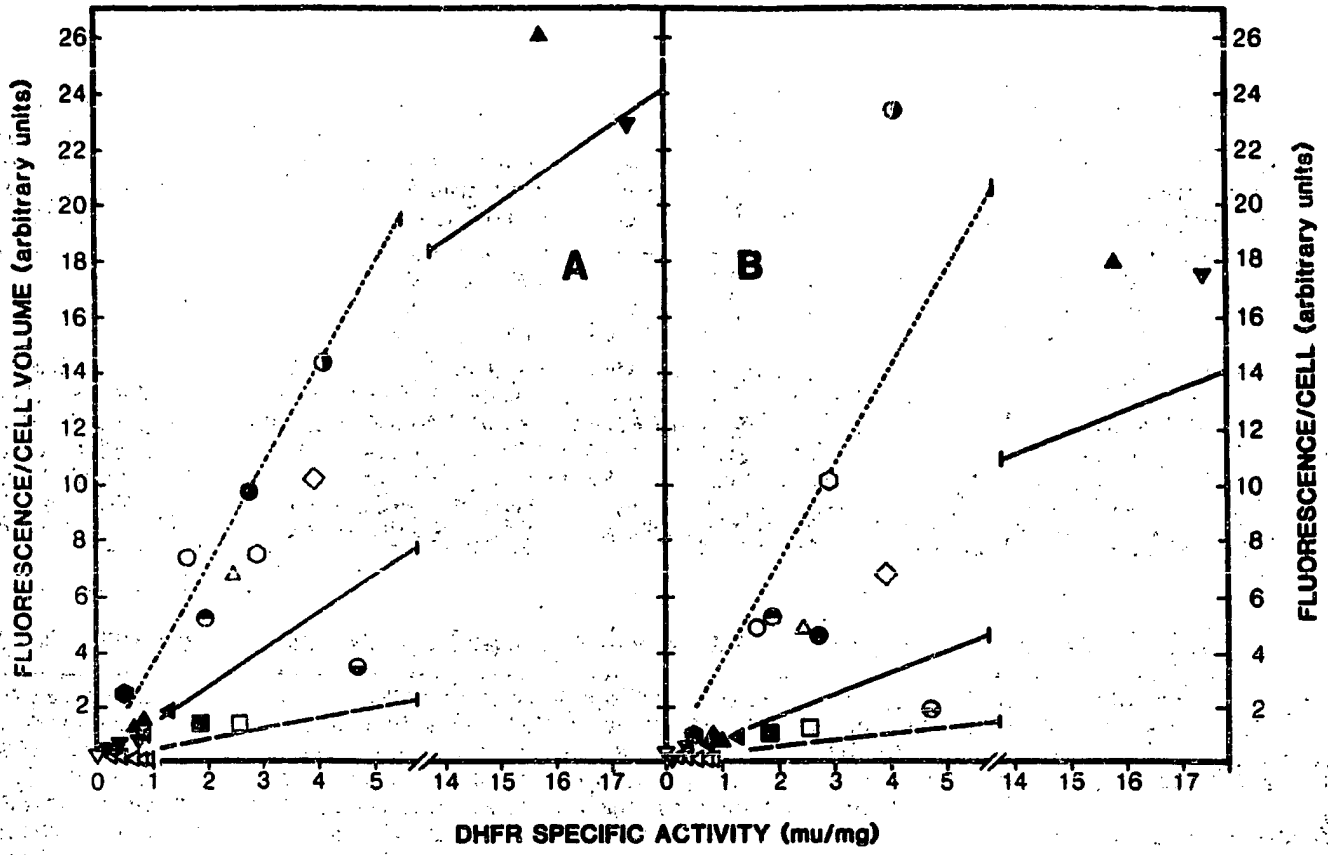


FIG. 5. **Correlation between Fluo-MTX labeling of various cell lines and their content of dihydrofolate reductase enzyme.** Cells were labeled with 1 μM Fluo-MTX and analyzed by flow cytofluorometry according to "Materials and Methods." Relative cell volumes were calculated on the basis of the light scatter parameter. Parallel cultures were harvested the same day and cell extracts were prepared and dihydrofolate reductase activity was determined (see "Materials and Methods"). Hamster cells: △, CHO-K1 cells; ▽, DG44 (see "Materials and Methods"); ▲, DG44 transformed by pSV2-DHFR (Lee *et al.*, 1981); ▼, DG44 transformed by pPP-DHFR-2 (Fig. 1); ◀, DG44 transformed by pPDC-2 or pCDP-12 (Fig. 1); ◁, DXB-11 transformed by pCDP-12 (Fig. 1); ◁, DXB-11 transformed by pDP-1 (Fig. 1). Mouse cells: ○, ψ2 NIH-3T3 fibroblasts (Mann *et al.*, 1983); ⊖, 3T6 fibroblasts (Todaro and Green, 1963); ◑, S180 fibroblasts (Foley *et al.*, 1960); ⊖, BW5147 lymphocytes (Hyman and Stallings, 1974); ⊖, W7-TG lymphocytes (Bourgeois and Newby, 1977). Fisher rat cells: ▣, FR3T3 (Seif and Cuzin, 1977); □, 209-F (Quade, 1979). Other cells: ◇, CCL64 mink cells (Henderson *et al.*, 1974); ◈, PA101 chicken myoblasts (Montarras and Fizman, 1983); ○, COS monkey cells (Gluzman, 1981); ●, CEM human lymphocytes (Foley *et al.*, 1965). The *dashed*, *dotted*, and *continuous lines* correspond to the least square regressions of rat cells, mouse cells (with the exception of W7-TG), and DG44 transformants, respectively. The *ordinate* in *panel A* is the difference between the means of the specific fluorescence per cell volume in cells labeled with Fluo-MTX alone and in cells labeled with Fluo-MTX plus free MTX. In *panel B*, it is the difference between the means of total fluorescence without correction for cell volume in cells labeled with Fluo-MTX alone and in cells labeled with Fluo-MTX plus MTX.

result indicates that DXB11 cells, which have been obtained after intensive mutagenesis, carry an additional mutation which impairs transport of Fluo-MTX. Uptake of free MTX in these cells may be normal, as it has been shown that MTX and Fluo-MTX enter the cells via different routes (Hendereon *et al.*, 1980). Our observation is relevant to studies on expression of donated dihydrofolate reductase genes since the most commonly used recipient cell line is, in fact, DXB11.

Most of the studies on transient expression have been performed on genes encoding an enzyme which can be assayed *in vitro* (*e.g.* chloramphenicol acetyltransferase). In such cases, the level of expression is averaged for the total cell population although only a fraction of the cells in the population expresses the donated gene. Moreover, it is a common observation that the efficiency of transformation varies between experiments and between different transformations in the same experiment. Flow cytometry which analyzes a fluorescent signal on a cell by cell basis and gives at the same time the signal intensities of the different subpopulations, could prove to be a valuable method for the rapid and sensitive determination of factors affecting gene expression.

*Acknowledgments*—The advice and expert assistance of Jean Rivier and Susan Hochschwender in the synthesis, purification, and HPLC analysis of Fluo-MTX are gratefully acknowledged. We thank John M. Whiteley and Robert T. Schimke for giving us samples of Fluo-MTX, all our colleagues who provided us with the cell lines used in this study, Judy Meinkoth for a critical reading of the manuscript, and Marijke ter Horst and Karen Hyde for the preparation of this manuscript.

## REFERENCES

Alt, F., Kellems, R. E., Bertino, J. R., and Schimke, R. T. (1978) *J. Biol. Chem.* **253**, 1357–1370
Bishop, J. M. (1983) *Annu. Rev. Biochem.* **52**, 301–354
Bourgeois, S., and Newby, R. F. (1977) *Cell* **11**, 423–430

Bradford, M. M. (1976) *Anal. Biochem.* **72**, 248–254
Crouse, G. F., McEwan, R. N., and Pearson, M. L. (1983) *Mol. Cell. Biol.* **3**, 257–266
Foley, G. E., Drulet, B. P., McCarthy, R. E., Goulet, K. A., Dokos, J. M., and Filler, D. A. (1960) *Cancer Res.* **20**, 930–939
Foley, G. E., Lazarus, H., Farber, S., Urzman, B. G., Boone, B. A., and McCarthy, R. E. (1965) *Cancer (Phila.)* **18**, 522–529
Frearson, P. M., Kit, S., and Dubbs, D. R. (1966) *Cancer Res.* **26**, 1653–1660
Gapski, G. R., Whiteley, J. M., Rader, J. I., Cramer, P. L., Henderson, G. B., Neef, V., and Huennekens, F. M. (1975) *J. Med. Chem.* **18**, 526–528
Gluzman, Y. (1981) *Cell* **23**, 175–182
Hakala, M. T., Zabrzewski, S. F., and Nichol, C. A. (1961) *J. Biol. Chem.* **236**, 952–958
Henderson, C., Lieber, M. M., and Todaro, G. J. (1974) *Virology* **60**, 282–284
Henderson, G. B., Russel, A., and Whiteley, J. M. (1980) *Arch. Biochem. Biophys.* **202**, 29–34
Kyman, R., and Stallings, V. (1974) *J. Natl. Cancer Inst.* **52**, 429–436
Johnston, R. N., Beverley, S. M., and Schimke, R. T. (1983) *Proc. Natl. Acad. Sci. U. S. A.* **80**, 3711–3715
Kaufman, R. J., Bertino, J. R., and Schimke, R. T. (1978) *J. Biol. Chem.* **253**, 5852–5860
Lee, F., Mulligan, R., Berg, P., and Ringold, G. (1981) *Nature* **294**, 228–232
Mann, R., Mulligan, R. C., and Baltimore, D. (1983) *Cell* **33**, 153–159
Mariani, B. D., and Schimke, R. T. (1984) *J. Biol. Chem.* **259**, 1901–1910
Milbrandt, J. D., Heintz, N. H., White, W. C., Rothman, S. M., and Hamlin, J. L. (1981) *Proc. Natl. Acad. Sci. U. S. A.* **78**, 6043–6047
Montarras, D., and Fiszman, M. Y. (1983) *J. Biol. Chem.* **258**, 3883–3888
Pall, M. (1981) *Proc. Natl. Acad. Sci. U. S. A.* **78**, 2465–2468
Poustka, A. M., Rackwitz, H. R., Frischauf, A. M., Hohn, B., and Lehrach, H. (1984) *Proc. Natl. Acad. Sci. U. S. A.* **81**, 4129–4133
Quade, K. (1979) *Virology* **98**, 461–465
Rosowsky, A., Wright, J. E., Shapiro, H., Beardsley, P., and Lazarus, H. (1982) *J. Biol. Chem.* **257**, 14162–14167
Schimke, R. T. (1982) *Gene Amplification*, Cold Spring Harbor Laboratory, Cold Spring Harbor, NY
Schimke, R. T. (1984) *Cancer Res.* **44**, 1735–1742
Seif, R., and Cuzin, F. (1977) *J. Virol.* **24**, 721–728
Shen, Y. M., Hirschhorn, R. R., Mercer, W. E., Surmacz, E., Tsutsui, Y., Soprano, K. J., and Baserga, R. (1982) *Mol. Cell. Biol.* **2**, 1145–1154
Stark, G. R., and Wahl, G. M. (1984) *Annu. Rev. Biochem.* **53**, 447–491
Todaro, G. J., and Green, H. (1963) *J. Cell. Biol.* **17**, 299–313
Urlaub, G., and Chasin, L. A. (1980) *Proc. Natl. Acad. Sci. U. S. A.* **77**, 4216–4220
Urlaub, G., Käas, E., Carothers, A. M., and Chasin, L. A. (1983) *Cell* **33**, 405–412
Wahl, G. M., Robert de Saint Vincent, B., and DeRose, M. L. (1984) *Nature* **307**, 516–520

QH573.C95
W05

**STIC-ILL**

**From:** Gabel, Gailene
**Sent:** Monday, March 18, 2002 12:39 PM
**To:** STIC-ILL
**Subject:** 09/752,453

387742

Please provide a copy of the following literature:

1) Gaudray et al "Fluorescent Methotrexate Labeling and Flow-Cytometric Analysis . . . " J. Biol. Chem. 261:6285-6292 (May 1986).

2) Morris, G. et al., "Cysteine Proteinase Inhibotors And Bleomycin-Sensitive And -Resistant Cells", Biochemical Pharmacology, vol. 41, No. 11, pp. 1559-1566, 1991.

3) Herweijer et al., A Rapid and Sensitive Flow Cytometric Method for the Detection of Multidrug-Resistant Cells," Cytometry, 10: 463-468,(1989).

Thanks a bunch!!!

Gail Gabel
7B15
CM1
305-0807

AgL
3/19
SMP
Completed
0
7
.63

The Journal of the Society for Analytical Cytology

# CYTOMETRY

Volume 10, Number 4, July 1989

Alan R. Liss, Inc., New York

Cytometry 10:463–468 (1989)

# A Rapid and Sensitive Flow Cytometric Method for the Detection of Multidrug-Resistant Cells[1,2]

**Hans Herweijer, Ger van den Engh,[4] and Kees Nooter[3]**
Daniel den Hoed Cancer Center, Rotterdam and Radiobiological Institute TNO, 2280 HV Rijswijk, The Netherlands

Received for publication October 25, 1988; accepted February 27, 1989

**Multidrug-resistant (MDR) cells are characterized by a defect in drug accumulation caused by activity of an energy-dependent rapid drug efflux pump. The action of this drug pump can be inhibited by specific agents, referred to as membrane transport modulating agents (MTMAs), resulting in a restoration of the intracellular drug accumulation. This paper presents a flow cytometric assay for the detection of MDR cells, which is based on the ability of these cells to respond to MTMAs. Daunorubicin net-uptake kinetics were measured of anthracycline-sensitive (A2780/S) and -resistant (A2780/R) human ovarian carcinoma cells in vitro. A2780/R cells accumulated significantly less (about a factor of 5) daunorubicin as compared to A2780/S cells. Addition of verapamil or cyclosporin A to A2780/R cells at steady-state daunorubicin uptake led to a dose-dependent increase in cellular daunorubicin accumulation. The sensitivity of the assay was determined by testing mixtures of A2780/S and A2780/R cells. Analysis of A2780/S cells contaminated with A2780/R cells showed that as few as 2.5% MDR cells could readily be detected in the mixture. In conclusion, this functional assay enables the detection of MDR cells in a heterogeneous cell suspension and is ideally suited for the study of the occurrence of typical MDR in human cancer.**

**Key terms: Multidrug resistance, MDR, flow cytometry, FCM, anthracyclines, kinetics of uptake, P-170 glycoprotein, daunorubicin**

Mammalian cell lines that have been selected in vitro for resistance to cytotoxic drugs such as the Vinca alkaloids or the anthracycline antibiotics display the so-called multidrug-resistant (MDR) phenotype. Several different MDR phenotypes have been described, which can be divided into two categories: typical (classical) MDR and atypical (variant) MDR (see ref. 2 for a review). Typical MDR is a rather well-defined phenotype that is characterized by a crossresistance to other structurally unrelated anticancer drugs and a decreased drug accumulation because of enhanced drug efflux. The molecular basis of typical MDR is an expression of a membrane-bound 170 kD glycoprotein, P-170 (8,16,20). P-170 functions as a drug efflux pump (7), and overexpression of P-170 leads to an increased drug extrusion, effectively lowering the intracellular drug concentration. By exposure to a variety of substances, such as calcium channel blockers and calmodulin antagonists, intracellular drug accumulation is increased, and drug sensitivity is restored (5,19). The current hypothesis about reversing MDR for some of these agents (e.g., verapamil) is that they have an affinity for P-170 and thus can compete for outward transport and thereby restore the cellular cytotoxic drug accumulation. For that reason the MDR-reversing agents are here referred to as membrane transport-modulating agents—MTMAs.

There is accumulating evidence that MDR can also occur in human cancer (1,4,6). This is potentially of therapeutic importance, since MTMAs have been found to overcome MDR in in vivo model systems (17). Therefore, it is of great importance to determine the occurrence of MDR in human cancer. Thus, accurate, sensitive, and rapid assays for the detection of MDR cells are highly desirable. In this paper the development of a

[1]This work was supported by KWF-Netherlands Cancer Foundation, grant number RRTI 88-08.

[2]This work was presented in part at the XIII International Meeting of the Society for Analytical Cytometry, Breckenridge, CO, September 4–9, 1988.

[3]Address reprint requests to K. Nooter, Radiobiological Institute TNO, P.O. Box 5815, 2280 HV Rijswijk, The Netherlands.

[4]Ger van den Engh is now at Lawrence Livermore National Laboratory-Biomedical Sciences Division, Livermore, CA 94550.

flow cytometric assay for the detection of MDR cells in heterogeneous cell populations is reported. The assay is based on the unique feature of typical MDR cells to increase drug accumulation upon the addition of MTMAs.

## MATERIALS AND METHODS

### Cells

The human ovarian carcinoma cell line A2780 (3), and its 100-times anthracycline-resistant mutant 2780AD (10) were used. Both cell lines were kindly supplied by Drs. R.F. Ozols and T.C. Hamilton (National Cancer Institute, Bethesda, MD). The anthracycline-sensitive A2780 cells and the anthracycline-resistant 2780AD cells are referred to by us as A2780/S and A2780/R, respectively. Cells were grown in plastic flasks in RPMI 1640 (Gibco, Paisley, Scotland), supplemented with 10% (v/v) fetal calf serum (Sera-Lab, Sussex, England) at 37°C in a humidified atmosphere of 5% $CO_2$ in air. The A2780/R cells were continuously challenged with 2 μM daunorubicin. Prior to flow cytometric analysis, the A2780/R cells were cultured in drug-free medium for 48 hours. Cells were harvested, washed twice with HEPES-buffered Hanks' balanced salt solution (HHBSS, pH 7.4), and resuspended in HHBSS to a final concentration of $2 \times 10^5$ cells/ml. A2780/R cells showed amplification of the MDR gene and overexpression of MDR mRNA and P-170 glycoprotein (ref. 10; and own observations).

### On-Line Flow Cytometry

The RELACS-III flow cytometer was modified to allow for real-time measurements of the cellular daunorubicin uptake. An extensive description of our on-line flow cytometric technique is given in reference 11 (it is very well possible to perform the measurements of net-uptake kinetics as described in this paper with other commercially available systems). The cells were kept at 37°C in a reaction vessel (Falcon 2025 tubes, Becton Dickinson Labware, Lincoln Park, NJ), which is surrounded by a thermostated water jacket. The vessel is connected to the flow cuvette of the RELACS-III. By means of air pressure the medium containing the cells is forced through the flow cuvette. An extra inlet in the reaction vessel allows for the addition of drug, while monitoring the daunorubicin content of the cells (11,12). The method makes use of the fluorescent properties of the anthracyclines. The excitation laser (Coherent Innova 90-5, Palo Alto, CA) is tuned to emit 0.6 W of 488 nm light. This wavelength is close to the absorption maximum of daunorubicin. The cells were analyzed at a rate of 500–1,000 cells per second. Per cell, four signals were digitized and stored as data list in a computer (21). The measured parameters were forward and perpendicular light scatter, forward light scatter pulse width, and daunorubicin fluorescence. The scattering parameters were used to gate out debris, dead cells, and cell clumps. Scattering light was filtered through 488 nm band pass filters (Melles Griot, Irvine, CA) and linearly amplified. Daunorubicin fluorescence was filtered through a 550 nm long pass filter (Schott, Mainz, FRG), and logarithmically amplified. On predetermined times the data of 2,000 cells were stored. It was possible to take one sample per 2 seconds. In addition to the normal pulse height processing electronics the system contains a timer that is read periodically (10 times per second) (21). The time marks are placed in between the list mode data and can therefore be used to construct accurate kinetic curves. The means and standard error of the daunorubicin fluorescence intensity of specific cell populations, as characterized by scattering parameters, can be computed afterward and plotted versus the sampling time, thus creating net-uptake curves. In these calculations, the logarithmically measured fluorescence intensity is recalculated to the linear value. The flow cytometer was aligned with fluorescent beads (Polysciences, Warrington, PA), and the photomultiplier voltage was adjusted to have the modal fluorescence always in the same channel, thus enabling measurements on different days to be compared with each other.

### Quantification of Daunorubicin by HPLC

Intracellular daunorubicin and daunorubicinol concentrations were determined by high-performance liquid chromatography (HPLC) as described previously (13). Experiments were carried out in quadruplicate.

### Chemicals

Daunorubicin (Cerubidin®) was obtained from Rhône-Poulenc, Paris. Verapamil (Isoptin®) and cyclosporin A (Sandimmune®) were purchased from Knoll, Ludwigshafen, FRG and Sandoz, Basel, Switzerland, respectively.

## RESULTS

### On-Line Flow Cytometry

With a flow cytometer, the in vitro uptake of anthracyclines by cells can be measured (9,12,14,15,18). The on-line flow cytometric technique described in this paper allows for the determination of the kinetics of net-uptake of anthracyclines by cells. The first data point in these kinetic measurements is taken before addition of daunorubicin to the sample. After storing of these data, daunorubicin is added to the sample tube. The time intervals between the data points are set up logarithmically, resulting in many data points shortly after addition of the drug, enabling accurate construction of uptake curves. Figure 1 shows the kinetics of daunorubicin uptake by A2780/S and A2780/R cells as measured with on-line flow cytometry. Uptake measurements were performed over a time period of 90 minutes. Steady-state kinetics were reached after approximately 60 and 30 minutes for sensitive A2780/S and resistant A2780/R cells, respectively. Sensitive

FIG. 1. D
a.u.) of A278
= 0, daunor
bated at 37°C

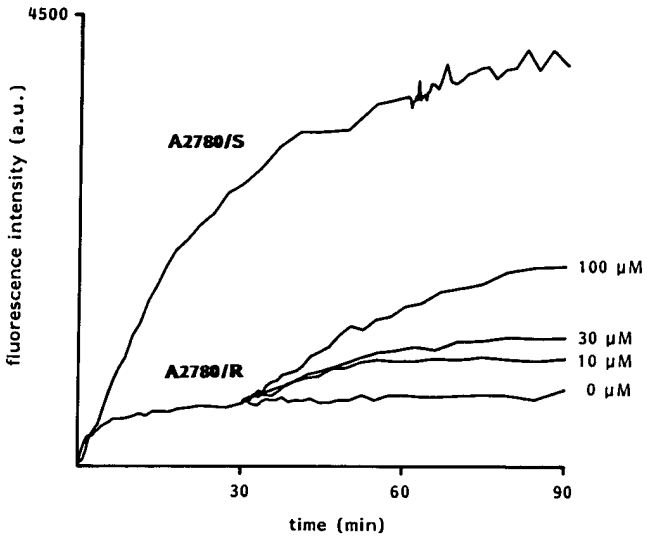


FIG. 1. Daunorubicin fluorescence intensity (in arbitrary units, a.u.) of A2780/S and A2780/R cells vs. the drug exposure time. At time = 0, daunorubicin (2 μM) was added to the cells, which were incubated at 37°C. After 30 minutes, verapamil was added to the A2780/R cells. Daunorubicin net-uptake was measured for another 60 minutes. Several samples were measured, to which different concentrations of verapamil were added. After 60 minutes, HHBSS was added as control to the A2780/S cells.

A2780/S cells reached a steady-state level of approximately five times the level of resistant A2780/R cells.

Addition of the MTMA verapamil to samples of A2780/R cells incubated with daunorubicin for 30 minutes resulted in a dose-dependent increase in the intracellular daunorubicin concentration over a time period of 60 minutes (Fig. 1). The same type of modulation was observed after addition of another MTMA: cyclosporin A (Fig. 2). Full restoration of daunorubicin uptake could not be obtained by addition of either modulator, even after addition of 100 μM verapamil (Fig. 1) or 10 μM cyclosporin A (Fig. 2). Addition of MTMAs to the sensitive A2780/S cells did not result in changes in the daunorubicin accumulation.

### Quantification of Daunorubicin by HPLC

To prove that the measured increases in cellular daunorubicin fluorescence, as induced by verapamil or cyclosporin A, reflect true increases in daunorubicin accumulation, the intracellular drug concentrations have also been determined by HPLC (13). A2780/S and A2780/R cells were incubated with 2 μM daunorubicin for 60 minutes at 37°C. Thereafter MTMAs were added to the cell samples, and the incubations were continued for another 60 minutes. The cells were spun down, and the intracellular daunorubicin concentrations were determined. The results are shown in Table 1. The drug concentrations in the sensitive A2780/S cells were about fivefold higher than in the resistant A2780/R cells. Both verapamil and cyclosporin A reversed the MDR phenotype of the A2780/R cells, resulting in increased intracellular drug concentrations, which corresponded with simultaneous flow cytometric determinations. No effect of MTMA addition to A2780/S cells was measured. In the A2780/S cells as well as in the A2780/R cells no metabolites of daunorubicin were detected by HPLC.

### Sensitivity of the On-Line Flow Cytometric MDR Assay

To obtain an indication of the sensitivity of the on-line flow cytometric assay for the detection of MDR cells, mixing experiments were performed. Sensitive A2780/S and resistant A2780/R cells were mixed in different ratios, and subsequently the daunorubicin uptake kinetics and modulation by cyclosporin A were measured. Plotting of the fluorescence histograms measured at several time points after addition of daunorubicin allowed for the detection of small subpopulations of MDR cells. Figure 3A shows the histograms of the daunorubicin uptake of a 1:1 mix of sensitive and resistant A2780 cells over a time period of 60 minutes. The increase in fluorescence of both cell types can be seen, as well as the differences between sensitive and resistant cells. The effects of the addition of 10 μM cyclosporin A are shown in Figure 3B. The sensitive cells retained the same fluorescence level, while the resistant cells started accumulating daunorubicin again. After about 60 minutes, the peaks of the sensitive and resistant cells merged on these histograms with logarithmic scale. The effects of cyclosporin A addition to samples of A2780/S cells containing 10% and 2.5% A2780/R cells are shown in Figure 3C and 3D, respectively.

## DISCUSSION

The data presented in this paper show that on-line flow cytometry allows for the measurement of drug

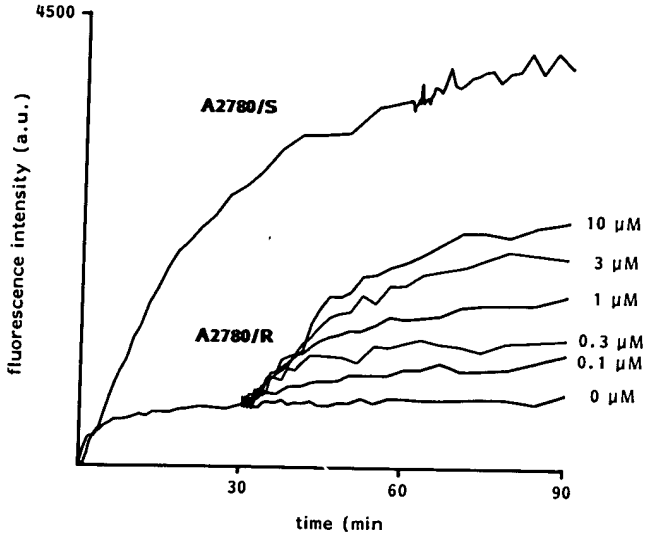


FIG. 2. For explanations see Figure 1. However, cyclosporin A now was added to the A2780/R samples in different concentrations after 30 minutes.

Table 1
*Intracellular Daunorubicin Concentrations in A2780/S and A2780/R Cells, as Determined by HPLC*

| Incubation with (μM)[a] | | | Daunorubicin concentration[b] | |
|---|---|---|---|---|
| Daunorubicin | Verapamil | Cyclosporin A | A2780/S | A2780/R |
| 2 | — | — | 533 ± 100 | 108 ± 13 |
| 2 | 100 | — | 531 ± 58 | 252 ± 18 |
| 2 | — | 10 | 604 ± 71 | 297 ± 21 |

[a]A2780 cells ($0.4 \times 10^6$/ml) were incubated at 37°C for 60 minutes with daunorubicin. Thereafter verapamil, cyclosporin A, or medium was added, and the cells were incubated for another 60 minutes. The cells were spun down, and the intracellular daunorubicin concentrations were determined by HPLC.
[b]Expressed as μg ± SD per $10^9$ cells.

uptake kinetics, starting from the time of addition of the drug up to a few hours thereafter, using only one sample. Because of the frequent sampling of data points, accurate net-uptake curves are obtained. With this assay, the effects of the addition of MTMAs can be followed satisfactorily. The increased intracellular daunorubicin concentrations in A2780/R cells, induced by addition of verapamil or cyclosporin A, as estimated by flow cytometry, could be confirmed by HPLC.

The assay described here for the detection of multidrug-resistant cells has the advantage over biochemical methods in that it is a functional assay of P-170 glycoprotein activity: only cells that can respond to MTMA's are scored as MDR cells. This is especially of importance when patient treatment is being considered with drugs that can potentially overcome MDR. It is obvious that it only makes sense to treat those drug-resistant cancer patients whose tumor cells do react to MTMAs in vitro. Another advantage of this on-line flow cytometric assay is that it allows for an estimation of the size of MDR cell clones in heterogeneous populations. Even the presence of a very small number of drug-resistant A2780/R cells (as low as 2.5%) could be detected within a population of drug-sensitive A2780/S cells. The assay allows for the detection of small increases in daunorubicin accumulation of about 10%, as was measured for the resistant A2780/R cells upon the addition of low concentrations of MTMAs. Therefore, it seems likely that this assay is also suited for the detection of lowly resistant cells, as might be the case in human tumor cell populations.

For the human ovarian carcinoma A2780/R cells, cyclosporin A appeared to be far more effective, on a molar basis, in restoring daunorubicin accumulation than verapamil. In a previous study (12), using the mouse P388 MDR cell line, cyclosporin A and verapamil were equally effective in that respect. Whether these differences reflect species differences remains to be investigated further.

In conclusion, on-line flow cytometry is a promising method for the study of the occurrence of multidrug-resistant cells in human cancer, and it allows for reliable in vitro evaluation of combination therapy of anthracycline drugs and MTMAs.

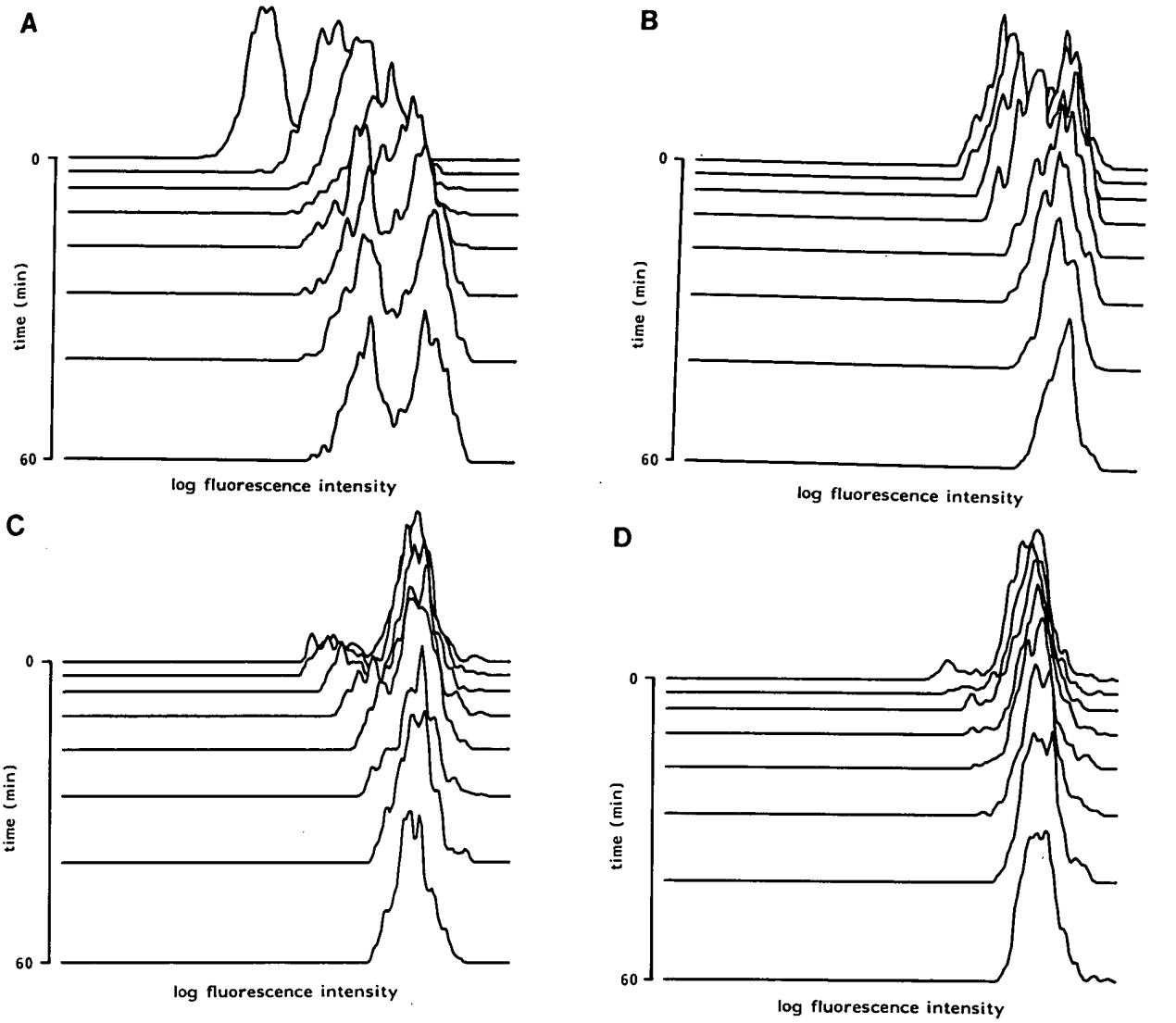


FIG. 3. Histograms of daunorubicn fluorescence intensity (logarithmic scale) of mixtures of A2780/S and A2780/R cells measured at several drug exposure times, plotted in front of each other. **A:** 1:1 mixture of sensitive and resistant cells. At time = 0, daunorubicin (2 μM) was added to the cells, which were incubated at 37°C. Daunorubicin accumulation was measured for 60 minutes. **B:** 1:1 mixture of sensitive and resistant cells. Cells were incubated with daunorubicin (2 μM) at 37°C for 60 minutes, prior to addition of 10 μM cyclosporin A at time = 0. Daunorubicin accumulation was measured for another 60 minutes. **C:** Same as B, with a 9:1 mixture of sensitive and resistant cells. **D:** Same as B, with a 24:1 mixture of sensitive and resistant cells.

## ACKNOWLEDGMENTS

We gratefully acknowledge Mr. A.W.M. Boersma and Mr. A.J. de Vries for excellent technical assistance.

## LITERATURE CITED

1. Bell DR, Gerlach JH, Kartner N, Buick RN, Ling V: Detection of P-glycoprotein in ovarian cancer: A molecular marker associated with multidrug resistance. J Clin Oncol 5:311–315, 1987.
2. Bradley G, Juranka PF, Ling V: Mechanism of multidrug resistance. Biochim Biophys Acta 948:87–128, 1988.
3. Eva A, Robbins KC, Anderson PR, Srinivasan A, Tronick SR, Reddy EP, Ellmore NW, Galen AT, Lautenberger JA, Papas TS, Westin EH, Wong-Staal F, Gallo RC, Aaronson SA: Cellular genes analogous to retroviral onc genes are transcribed in human tumour cells. Nature 295:116–119, 1982.
4. Fojo AT, Ueda K, Slamon DJ, Poplack DG, Gottesman MM, Pastan I: Expression of a multidrug-resistance gene in human tumors and tissues. Proc Natl Acad Sci USA 84:265–269, 1987.
5. Ganapathi R, Grabowski D, Turinic R, Valenzuela R: Correlation between potency of calmodulin inhibitors and effects on cellular levels and cytotoxic activity of doxorubicin (Adriamycin) in resistant P388 mouse leukemia cells. Eur J Cancer Clin Oncol 20: 799–806, 1984.
6. Gerlach JH, Bell DR, Karakousis C, Slocum HK, Kartner N, Rustum YM, Ling V, Baker RM: P-glycoprotein in human sarcoma: Evidence for multidrug resistance. J Clin Oncol 5:1452–1460, 1987.
7. Gerlach JH, Endicott JA, Juranka PF, Henderson G, Sarangi F, Deuchars KL, Ling V: Homology between P-glycoprotein and bacterial haemolysin transport proteins suggests a model for multidrug resistance. Nature 324:485–489, 1986.

8. Gros P, Neriah YB, Croop JM, Housman DE: Isolation and expression of a complementary DNA that confers multidrug resistance. Nature 323:728–731, 1986.
9. Krishan A, Ganapathi R: Laser flow cytometric studies on intracellular fluorescence of anthracyclines. Cancer Res 40:3985–3990, 1980.
10. Louie KG, Hamilton TC, Winkler MA, Behrens BC, Tsuruo T, Klecker RW, McKoy WM, Grotzinger KR, Myers CE, Young RC, Ozols RF: Adriamycin accumulation and metabolism in adriamycin-sensitive and -resistant human ovarian cancer cell lines. Biochem Pharmacol 35:467–472, 1986.
11. Nooter K, Herweijer H, Jonker RR, van den Engh GJ: On-line flow cytometry—a versatile method for kinetic measurements. In: Methods in Cell Biology, Volume 33: Flow Cytometry, Darzynkiewicz Z, Crissman HA (eds). Academic Press, San Diego, CA, in press.
12. Nooter K, Oostrum R, Jonker RR, van Dekken H, Stokdijk W, van den Engh GJ: Effect of cyclosporin A on daunorubicin accumulation in multidrug-resistant P388 leukemia cells measured by real-time flow cytometry. Cancer Chemother Pharmacol 23:296–300, 1989.
13. Nooter K, Sonneveld P, Martens A, Hagenbeek A, Schultz F: Tissue distribution and myelotoxicity of daunomycin in the rat: Bolus injection vs continuous infusion. Eur J Cancer Clin Oncol 22:801–806, 1986.
14. Nooter K, van den Engh GJ, Sonneveld P: Quantitative flow cytometric determination of anthracycline content of rat bone marrow cells. Cancer Res 43:5126–5130, 1983.
15. Ross DD, Ordóñez JV, Joneckis CC, Testa JR, Thompson BW: Isolation of highly multidrug-resistant P388 cells from drug-sensitive P388/S cells by flow cytometry. Cytometry 9:359–367, 1988.
16. Shen DW, Fojo AT, Roninson IB, Chin JE, Soffir R, Pastan I, Gottesman MM: Multidrug resistance of DNA-mediated transformants is linked to transfer of the human mdr 1 gene. Mol Cell Biol 6:4039–4044, 1986.
17. Skovsgaard T, Danø K, Nissen NI: Chemosensitizers counteracting acquired resistance to anthracyclines and Vinca alkaloids in vivo. A new treatment principle. Cancer Treat Rev 11:63–72, 1984.
18. Sonneveld P, van den Engh GJ: Differences in uptake of adriamycin and daunomycin by normal BM cells and acute leukemia cells determined by flow cytometry. Leuk Res 5:251–257, 1981.
19. Tsuruo T, Iida H, Tsukagushi S, Sakurai Y: Increased accumulation of vincristine and adriamycin in drug-resistant tumor cells following incubation with calcium antagonists and calmodulin inhibitors. Cancer Res 42:4730–4733, 1982.
20. Ueda K, Cardarelli C, Gottesman MM, Pastan I: Expression of a full-length cDNA for the human "MDR 1" gene confers resistance to colchicine, doxorubicin and vinblastine. Proc Natl Acad Sci USA 84:3004–3008, 1987.
21. van den Engh GJ, Stokdijk W: A parallel data acquisition system for multilaser flow cytometry and cell sorting. Cytometry, in press.

RP901.05
Mic.
Adams

**STIC-ILL**

**From:** Gabel, Gailene
**Sent:** Monday, March 18, 2002 12:39 PM
**To:** STIC-ILL
**Subject:** 09/752,453

Please provide a copy of the following literature:

1) Gaudray et al "Fluorescent Methotrexate Labeling and Flow-Cytometric Analysis . . . " J. Biol. Chem. 261:6285-6292 (May 1986).

2) Morris, G. et al., "Cysteine Proteinase Inhibotors And Bleomycin-Sensitive And -Resistant Cells", Biochemical Pharmacology, vol. 41, No. 11, pp. 1559-1566, 1991.

3) Herweijer et al., A Rapid and Sensitive Flow Cytometric Method for the Detection of Multidrug-Resistant Cells," Cytometry, 10: 463-468,(1989).

Thanks a bunch!!!

Gail Gabel
7B15
CM1
305-0807

*Biochemical Pharmacology*, Vol. 41, No. 11, pp. 1559–1566, 1991
Printed in Great Britain.

0006-2952/91 $3.00 + 0.00


# CYSTEINE PROTEINASE INHIBITORS AND BLEOMYCIN-SENSITIVE AND -RESISTANT CELLS

GEOFFREY MORRIS, JEHANGIR S. MISTRY, JITESH P. JANI, SAID M. SETTI and JOHN S. LAZO*

Department of Pharmacology, University of Pittsburgh, School of Medicine, and the Experimental Therapeutics Program, Pittsburgh Cancer Institute, Pittsburgh, PA 15261, U.S.A.

(*Received* 20 *August* 1990; *accepted* 19 *November* 1990)

**Abstract**—We have isolated a new human head and neck carcinoma cell line (C-10E) that is highly resistant to BLM (40-fold) when compared to the parental (A-253) cell line. Consonant with BLM resistance in the C-10E cell line, we found that this cell line accumulated 2- to 3-fold less BLM $A_2$ than A-253 cells. Kinetic analyses of BLM $A_2$ association revealed a decreased $V_{max}$ for C-10E cells with little change in $K_a$. Furthermore, the BLM-resistant cell line (C-10E) metabolized BLM $A_2$ to a greater extent than its sensitive counterpart (A-253). Thus, compared to A-253 cells, the C-10E cells exhibited both decreased cellular association and increased metabolism of BLM. Synergistic cytotoxicity was seen when BLM was combined with either E-64 or leupeptin, cysteine proteinase inhibitors known to block BLM metabolism *in vitro*. E-64 inhibited the metabolism of BLM $A_2$ in both C-10E and A-253 cells, and cellular accumulation of radiolabeled BLM $A_2$ was increased by leupeptin or E-64 in only A-253 cells. These results suggest that both inhibition of drug metabolism and increased drug accumulation contribute to this synergism.

The bleomycins (BLM†) are a family of related glycopeptide antibiotics derived from *Streptomyces verticillus* [1] and used therapeutically against many solid tumors, including squamous cell carcinoma and malignant lymphoma [2]. The bleomycins are unusual among the cytotoxic anticancer drugs in that they exhibit very little myelosuppressive or immunosuppressive activity; this has led to their popularity, particularly for use in combination with other antineoplastic agents [3]. Unfortunately, one of the major obstacles to chemotherapy has been drug resistance [4]. In an effort to elucidate mechanisms underlying cellular resistance, several cultured cell lines with low levels of BLM resistance have been isolated and these have exhibited either decreased drug association, decreased DNA breakage, or increased drug inactivation [5–7]. With regard to metabolic inactivation, it has been suggested that cells may become resistant to BLM through changes in BLM hydrolase (BH) activity, an enzyme that converts BLM to the inactive metabolite, deamidobleomycin (dBLM; [7–10]).

Recently, BH was identified as a member of the cysteine proteinase family [10]. Cysteine proteinases have been implicated in several important cellular processes including proliferation, cellular migration, polarization and transformation [11–13]. With the advent of highly specific cysteine proteinase inhibitors, it is now feasible to examine directly the effects of enzyme inhibition on BLM metabolism.

E-64 contains an epoxide moiety and inactivates cysteine proteinase irreversibly [14], while leupeptin is a reversible inhibitor of cysteine proteinase [15]. Because of the potential role of BH in BLM resistance, interactions between BLM and inhibitors of this enzyme activity are of interest. We have demonstrated recently that E-64 potentiates the antitumor activity of BLM in human Burkitt's lyphoma xenografts in nude mice by inhibiting BLM metabolism *in vivo* [16]. Nishimura *et al.* [17] reported that E-64 increases the cytotoxic action of peplomycin, a BLM analog, in cultured Chinese hamster lung cells, concomitant with increasing the fraction of unmetabolized drug. It is assumed that inhibition of drug metabolism elevated cellular BLM content. The same laboratory found that either leupeptin or E-64 was effective in prolonging the life span of mice bearing Ehrlich ascites carcinoma cells treated with peplomycin [18]. Because BLM-resistant human tumor cells may have altered BLM metabolism, we have examined the nature of the interaction between cysteine proteinase inhibitors and BLM using a newly characterized, highly BLM-resistant human head and neck squamous cell carcinoma.

## MATERIALS AND METHODS

*Cells and reagents*. A-253 human head and neck epidermoid carcinoma cells were obtained from the

* To whom requests for reprints should be addressed at: E-1346 Biomedical Science Tower, Department of Pharmacology, University of Pittsburgh, School of Medicine, Pittsburgh, PA 15261.

† Abbreviations: BH, bleomycin hydrolase; BLM, bleomycin; dBLM $A_2$, deamidobleomycin $A_2$; DMSO, dimethyl sulfoxide; E-64, l-transepoxysuccinylleucylamido(4-guanidino)butane; FBS, fetal bovine serum; $IC_{50}$, concentration of drug which inhibits cell growth to 50% of control; $K_a$, association constant; MTT, 3-(4,5-dimethylthiazol-2-yl)-2,5-diphenyltetrazolium bromide; PBS, phosphate-buffered saline; Tris, tris-hydroxymethylaminomethane; and $V_{max}$, maximal velocity.

American Type Culture Collection (Rockville, MD) and were grown in McCoy's Medium (Gibco, Grand Island, NY) supplemented with 10% fetal bovine serum (HyClone, Logan, UT) as previously described [19]. Cells were maintained at 37° in a humidifed incubator with a 95% air, 5% $CO_2$ atmosphere. The C-10E (BLM-resistant) cell line was derived from C-10 cells [19] by stepwise increase in BLM concentration added to the cultures. This process required 24 months, at which time cell proliferation was unaffected by continuous culturing of cells in 70 ng/mL (50 nM) of BLM. E-64, leupeptin, MTT and DMSO were obtained from the Sigma Chemical Co. (St. Louis, MO). Vincristine sulfate was a gift from Eli Lilly (Indianapolis, IN). Bleomycin $A_2$ was purified from BLM (Blenoxane; Bristol-Myers Squibb Co., Wallingford, CT) as described previously [20]. [*S*-methyl-$^3$H]BLM $A_2$ (sp. act. 78.4 Ci/mmol) was purchased from DuPont NEN Research Products (Boston, MA).

*Growth inhibition studies*. The effects of agents on cellular proliferation were determined using the previously described MTT microculture assay [19]. Briefly, exponentially growing cells were rinsed with PBS and harvested by treatment with trypsin (0.125%, w/v) and centrifugation at 200 *g* for 2 min. The cell pellet was resuspended in McCoy's modified medium with 10% fetal bovine serum (FBS). Cells were counted with a hemacytometer and seeded at a density of 2000 per well in 100 μL volume into 96-well microtiter plates (Costar, Cambridge, MA) using a multi-channel pipet. After 3 hr, drugs (100 μL) were added in serial dilutions to the wells. Drug ratios were chosen to approximate equitoxic concentrations of antineoplastic agent and proteinase inhibitor. After 4 days of growth in the presence or absence of drug(s), the medium was replaced with 100 μL of MTT (1 mg/mL) in McCoy's modified medium with 10% FBS. The tetrazolium/formazan reaction was allowed to proceed for 3 hr at 37°, after which time the solution containing the unreacted MTT was removed and replaced with 100 μL DMSO. After 5 min of shaking to solubilize all dye, the absorbance at wavelength 540 nm was determined spectrophotometrically (Titertek Multiskan; Flow Laboratories, McClean, VA). To evaluate possible drug interactions, isobolograms were generated for each drug combination using the dose-effect software package obtained from Elsevier-BIOSOFT (Cambridge, U.K.; [21]). Each isobole point was obtained by interpolation from a separate experiment designed to determine the concentration–response for each drug separately and for the drug combination.

*Cellular drug association studies*. The effect of proteinase inhibitor pretreatment on cellular association of [$^3$H]BLM $A_2$ was determined by previously described methods [19]. Exponentially growing A-253 cells were preincubated at 37° with E-64 (2 mM) or leupeptin (2 mM) for 72 hr prior to exposure to 1 μM [$^3$H]BLM $A_2$ for various time intervals to ensure complete enzyme inhibition. Drug incubation was terminated by pipetting 100 μL of cell suspension into 10 mL of ice-cold PBS, followed by centrifugation at 12,000 *g* for 30 sec. The resulting cell pellet was resuspended and centrifuged through an oil–aqueous layer as previously described [19]. For kinetic analyses, cells were incubated with radiolabeled BLM $A_2$ for 30 sec; the concentration of BLM $A_2$ was varied from 3.33 to 100 μM, and the amount of radioactivity associated with the cellular fraction was calculated for each drug concentration. Binding studies were performed at 4° in the same manner as the drug association studies.

*Metabolism studies*. Exponentially growing A-253 and C-10E cells were preincubated with or without E-64 (2 mM) for 72 hr. After preincubation, control and E-64-pretreated cells were treated with 1 μM [$^3$H]BLM $A_2$ (0.50 μCi/mL; sp. act. 78.4 Ci/mmol) and further incubated for 1 or 4 hr. The radioactive medium was removed and the cells were washed twice with 10 mL of ice-cold PBS. Cells were then harvested by treatment with PBS containing trypsin (0.05%, w/v) and EDTA (2 mM) and centrifuged at 200 *g*. Cell pellets were washed once with 5 mL of ice-cold PBS and homogenized in 1 mL of 20 mM ice-cold Tris–HCl (pH 6.5). Proteins were precipitated with 6 M ice-cold trichloroacetic acid. After addition of an equal volume of 0.5 M tri-*n*-octylamine in 1,1,2-trichlorotrifluoroethane to the supernatant fraction, the aqueous phase was filtered through a 0.2 μm ACRO filter, concentrated, and subjected to reverse phase ion-pair HPLC analysis as described earlier [20].

## RESULTS

*Resistant cell line*. To address the problem of drug resistance at the cellular level, we developed a human cell line with a higher degree of resistance than previously reported [6, 7, 19, 22]. The C-10E cell line was generated from the previously described 4-fold BLM-resistant C-10 cell line (Materials and Methods), which was derived from the parental (A-253) cell line by mutagenesis and subsequent stepwise increase in BLM exposure [19]. The C-10E line displayed a 40-fold resistance when compared to A-253 cells over a wide range of BLM $A_2$ concentrations (Fig. 1). Table 1 summarizes the relative sensitivities

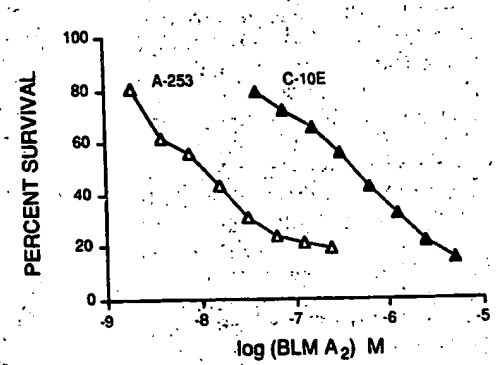


Fig. 1. Concentration–response of A-253 and C-10E cells to BLM. Cells were seeded in 96-well plates at a density of 2000 cells/well in 200 μL of McCoy's medium supplemented with 10% FBS. BLM was added after 2 hr and after 4 days the cell number was determined spectrophotometrically (540 nm) with MTT as described in Materials and Methods. Each point is the average of at least 24 determinations.

Table 1. Drug sensitivities of A-253 and C-10E cells

| Drugs | $IC_{50}$ (nM) A-253 | $IC_{50}$ (nM) C-10E | Resistance index |
|---|---|---|---|
| Bleomycin | 11 ± 0.5 | 440 ± 49 | 40* |
| Doxorubicin | 214 ± 4 | 194 ± 4 | 0.91 |
| Cisplatin | 1190 ± 79 | 460 ± 9 | 0.39† |
| Vincristine | 13 ± 0.5 | 15 ± 0.5 | 1.15 |

Cells were exposed to drugs for 4 days and growth inhibition was determined spectrophotometrically as described in Materials and Methods. The resistance index was calculated as the ratio of $IC_{50}$ for C-10E cells compared to the $IC_{50}$ for A-253 cells for each drug. Values are means ± SEM, N = 16 or more individual determinations.

*† Significant differences between A-253 and C-10E cells as determined by Student's *t*-test: * $P < 0.001$, and † $P < 0.05$.

of these two cell lines to a variety of anticancer drugs. Although C-10E cells were 40-fold resistant to BLM $A_2$, there was no cross-resistance to the structurally dissimilar antitumor drugs tested. C-10E cells also displayed some collateral sensitivity (2.6-fold) to cisplatin. Furthermore, the BLM-resistant phenotype was stable for 2 months in the absence of chronic BLM exposure after which time the cell line began to regain sensitivity to BLM (data not shown). The volume of both cells as measured using an electronic counter was similar for both cell lines (12–16 $\mu m^3$).

*Cellular association of* [$^3$H]*BLM* $A_2$. To evaluate one possible mechanism of resistance to BLM, we first investigated the importance of cellular drug association to the resistant phenotype. C-10E cells exhibited markedly less cellular association of BLM $A_2$ when compared to the sensitive A-253 cell line (Fig. 2A). After 10 min, the level of BLM $A_2$ associated with A-253 cells was nearly double that associated with C-10E cells; this difference increased so that at 30 min, when association plateaued for both cell lines, A-253 cells had nearly 3-fold more radioactivity than C-10E cells. A kinetic analysis of the initial cellular association (Fig. 2B and inset) revealed a higher $V_{max}$ for A-253 cells (183 pmol/$10^7$ cells/min) than for C-10E cells (105 pmol/$10^7$ cells/min) with no change in $K_a$ (75.0 vs 74.6 $\mu$M). At a concentration of 20 $\mu$M BLM $A_2$ there was a 50% blockade of association with 100-fold excess cold BLM $A_2$ (data not shown).

Binding of [$^3$H]BLM $A_2$ at 4° (Fig. 2C) also revealed a pattern similar to cellular association (Fig. 2A). Binding was rapid, with maximal cellular levels occurring within 20 min. The absolute values for binding were lower (approximately 0.5 to 0.25) than for cellular association of drug, and A-253 cells bound over 3-fold more [$^3$H]BLM $A_2$ than C-10E cells.

*Cellular metabolism of* [$^3$H]*BLM* $A_2$. We next determined the intracellular metabolism of BLM in sensitive and resistant phenotypes. Figure 3 shows the HPLC profiles of [$^3$H]BLM $A_2$ and its metabolites in intact A-253 and C-10E cells after various times of exposure to 1 $\mu$M [$^3$H]BLM $A_2$. After a 1-hr

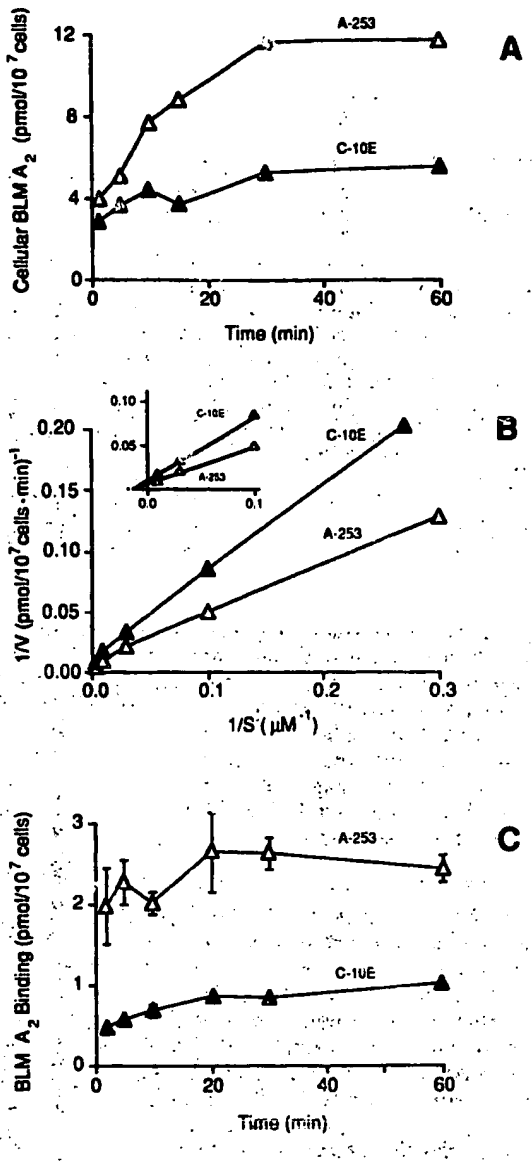


Fig. 2. (A) Cellular association of [$^3$H]BLM $A_2$ in A-253 and C-10E cells. Cells were exposed to 1 $\mu$M [$^3$H]BLM $A_2$ for various time intervals as described in Materials and Methods. Each point is the average of triplicate determinations. (B) Double-reciprocal plot of [$^3$H]BLM $A_2$ association in A-253 vs C-10E cells. For kinetic analyses, a single time of incubation with radiolabel of 30 sec was selected. The concentration of BLM $A_2$ ranged from 3.33 to 333.3 $\mu$M, and the assay for cellular association was performed as described in Materials and Methods. The equation for the best-fit line through the double-reciprocal graph (inset) was used to determine the $V_{max}$ and $K_a$ values for cellular drug association. The data are representative of two experiments. (C) Binding of [$^3$H]BLM $A_2$ in A-253 and C-10E cells. After cells were harvested, McCoy's medium chilled to 4° containing radioactive 1 $\mu$M [$^3$H]BLM $A_2$ was added. At various time intervals aliquots were removed, washed with ice-cold PBS, suspended in medium chilled to 4° and centrifuged at 9000 *g* in a microcentrifuge tube containing perchloric acid/silicone oil/mineral oil mixture. Each point is the average of six determinations; the SEM is included within the symbols unless noted by bars.

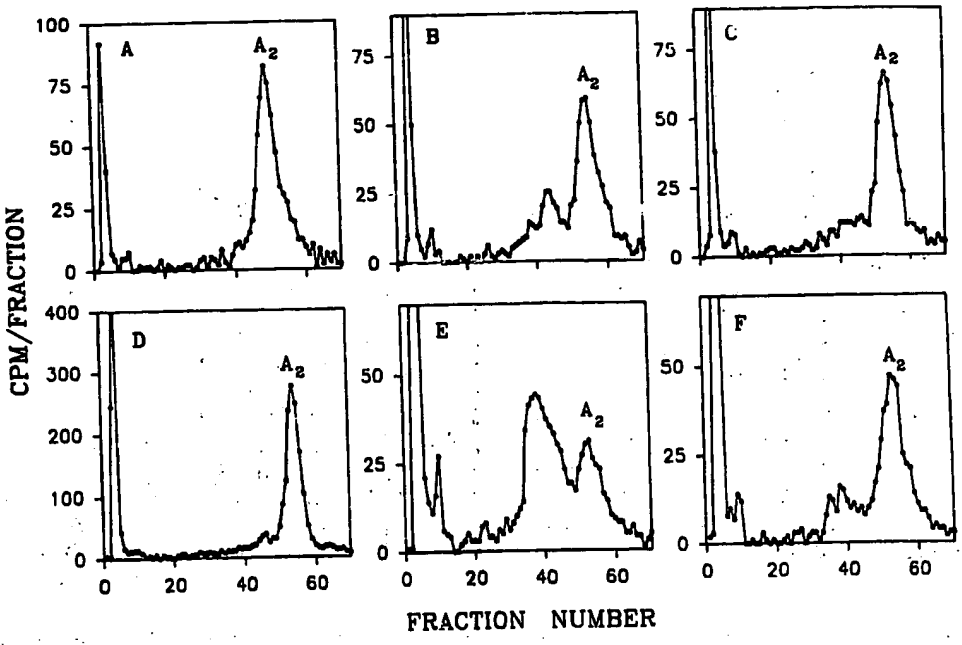


Fig. 3. Metabolism of [$^3$H]BLM $A_2$ in cultured A-253 and C-10E cells. A-253 cells (A, B and C) and C-10E cells (D, E and F) were treated with 1 $\mu$M [$^3$H]BLM $A_2$ for either 1 hr (A and D) or 4 hr (B, C, E and F). Prior to [$^3$H]BLM $A_2$ treatment the cells were incubated in the absence (B and E) or presence of 2 mM E-64 (C and F) for 72 hr. After BLM $A_2$ treatment all cells were harvested and homogenized, and the radioactivity was extracted as described in Materials and Methods. The radioactive material was then separated with a C-8 reverse phase HPLC column as described in Materials and Methods. The greatest cpm for each sample occurred in the solvent front and was: (A) 91.8 cpm, (B) 179 cpm, (C) 163 cpm, (D) 459 cpm, (E) 747 cpm and (F) 434 cpm. BLM $A_2$ designates the elution position of an authentic standard of BLM $A_2$.

incubation, there was little metabolism of drug by either cell line (Fig. 3, A and D). The only prominent peak seen other than BLM $A_2$ was found in the void volume (fractions 3–8) and was present in all samples at approximately the same percentage. After a 4-hr incubation with [$^3$H]BLM $A_2$, two additional peaks (fractions 9–11 and 36–45) were seen in A-253 cells (Fig. 3B); the majority of the retained radioactivity, however, remained in the unmetabolized BLM $A_2$ peak. In contrast, exposure of C-10E cells to [$^3$H]BLM $A_2$ for 4 hr resulted in more extensive metabolism and the majority of the radioactivity was in fractions 36–45, with a smaller peak corresponding to unmetabolized BLM $A_2$ (Fig. 3E). Based on the elution positions of authentic standards, dBLM $A_2$ (fractions 23–25), the only BLM $A_2$ metabolite that has been characterized, was not detected in either A-253 or C-10E cells. The chemical nature of these putative metabolites is not yet known due to small amounts that are available. It is interesting to note, however, that similar metabolites were suggested previously in non-malignant tissues *in vivo* [20], although they are much better resolved with our current HPLC methods. Our preliminary data indicate these metabolites are not able to degrade DNA [16].

*Drug interaction studies.* Because BLM is thought to be inactivated by a cysteine proteinase, BH, we next examined cell survival in the presence of both BLM and inhibitors of cysteine proteinases. Incubation of A-253 cells with concentrations of E-64 (2 mM) that alone failed to inhibit A-253 cell proliferation markedly increased the cytotoxicity of BLM ($IC_{50}$ = 88 nM in the absence of E-64; $IC_{50}$ = 44 nM in the presence of E-64). Thus, we formally examined whether E-64 or leupeptin could synergistically interact with BLM. Using drug concentration ratios to simulate roughly equitoxic concentrations of BLM and cysteine proteinase inhibitor, we generated isobolograms at the $IC_{50}$ level for each drug combination. With this model, we observed augmentation of cytotoxicity with combinations of BLM and cysteine proteinase inhibitors in both cell lines (Fig. 4). Points falling below the isoeffective ($IC_{50}$) line indicate enhancement of cytotoxicity created by the drug combination. The combination of E-64 and BLM $A_2$ resulted in enhanced cytotoxicity at both drug ratios tested in C-10E cells (Fig. 4A). Similarly, the combination of E-64 and BLM $A_2$ resulted in enhanced cytotoxicity at all ratios tested in A-253 cells (Fig. 4B). The combination of leupeptin and BLM $A_2$ resulted in synergism of cytotoxicity at the three ratios tested in A-253 cells (Fig. 4C).

*Cysteine proteinase and BLM $A_2$ metabolism and association.* Cysteine proteinase inhibitors, such as E-64, can block the metabolism of BLM by isolated BH [10]. We, therefore, examined the effect of E-64 pretreatment on BLM $A_2$ metabolism in intact cells. Preincubation of A-253 cells with E-64 (2 mM)

for 72 hr prior to [$^3$H]BLM $A_2$ completely abolished the major metabolite peak (fractions 36–45, Fig. 3C), with all radioactivity detected in either the BLM $A_2$ peak, fractions 9–11 or the void volume. Preincubation of C-10E cells with 2 mM E-64 for 72 hr (Fig. 3F) greatly reduced the radioactivity in fractions 36–45. When the percent of total radioactivity for each peak was calculated (Fig. 5), a similar pattern emerged. Peaks 1 (solvent front) and 2 (minor metabolite, fractions 9–11) were not changed by pretreatment with E-64 in either cell line. Peak 3 (major metabolite, fractions 36–45), however, was diminished substantially by E-64 pretreatment in both cell lines, with a corresponding increase in unmetabolized BLM $A_2$. Thus, E-64 was capable of blocking metabolism of BLM $A_2$ in both sensitive and resistant cell lines.

We next examined the effect of E-64 on cellular association of [$^3$H]BLM $A_2$ in the A-253 and C-10E cell lines. We did find a significant increase in [$^3$H]BLM $A_2$ association at all time points ($P < 0.005$) when A-253 cells were preincubated with 2 mM E-64 (Fig. 6A). The cellular association of radioactivity in the presence of E-64 was elevated approximately 2-fold and persisted for the full time-course of this study. Pretreatment with 2 mM leupeptin also resulted in a significant increase ($P < 0.05$) in cellular [$^3$H]BLM $A_2$ in A-253 cells at all time points (Fig. 6B). Association of [$^3$H]BLM $A_2$ was increased by nearly 2-fold during the first 30 min of incubation. Cellular association was rapid, peaked at 5 min, and declined slightly over the 60-min time-course. In contrast, E-64 pretreatment had no effect on cellular [$^3$H]BLM $A_2$ association in C-10E cells (Fig. 6C).

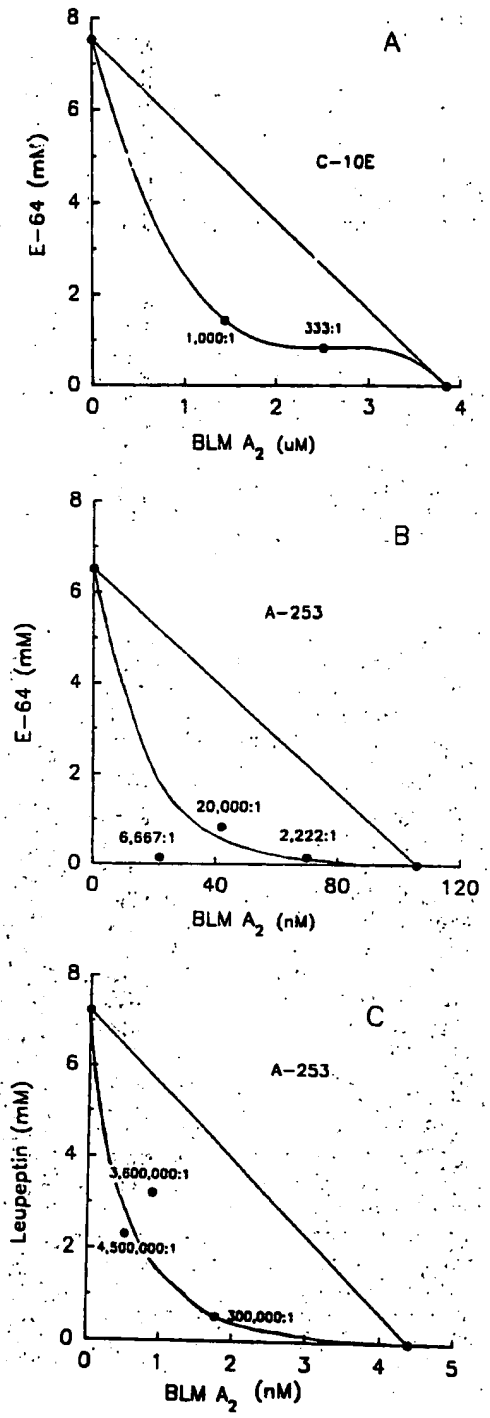


Fig. 4. Synergism with various ratios of cysteine proteinase inhibitors and BLM $A_2$ in A-253 and C-10E cells. Cells were seeded in microtiter plates and allowed to grow for 4 days in the presence of drug combinations. Cell number was determined spectrophotometrically (540 nm) after staining with MTT. Growth inhibition data were then transformed to $IC_{50}$ isobolograms using the median-effect software package obtained from Elsevier-BIOSOFT (U.K.). Each point is the mean value of three or more determinations, and drug ratios were chosen to bracket equitoxic doses for the two compounds. (A) Synergism with the drug combination of E-64 and BLM $A_2$ in C-10E cells. The molar drug ratios used were E-64:BLM $A_2$ of 1,000:1 and 333:1 as indicated. The $IC_{50}$ for E-64 alone in this experiment was 7.5 mM. (B) Synergism to the drug combination of E-64 and BLM $A_2$ in A-253 cells. Molar drug ratios used were E-64:BLM $A_2$ of 20,000:1, 6,667:1, or 2,222:1. The $IC_{50}$ for E-64 alone was 6.5 mM. (C) Synergism between leupeptin and BLM $A_2$ in the growth inhibition assay. A-253 cells were grown in the presence of molar drug ratios of 300,000:1, 3,600,000:1 or 4,500,000:1 for 4 days. The $IC_{50}$ for leupeptin in this experiment was 7.2 mM.

## DISCUSSION

We have developed a human squamous carcinoma cell line (C-10E), which is both highly (40-fold) and selectively resistant to BLM. The C-10E cells exhibit two phenotypic properties that distinguish them from the parental A-253 cells: (1) increased metabolism of BLM and (2) decreased cellular association of BLM. The BLM-resistant C-10E cells were not cross-resistant to doxorubicin or vincristine, but were more sensitive to cisplatin (Table 1). Thus, the C-10E cells have acquired a drug resistance profile distinct from cells previously derived from the parental A-253 cell line [19]. We find the collateral sensitivity of C-10E cells to cisplatin intriguing not because there is any apparent mechanistic basis but because BLM is often used with cisplatin and this could have some clinical significance.

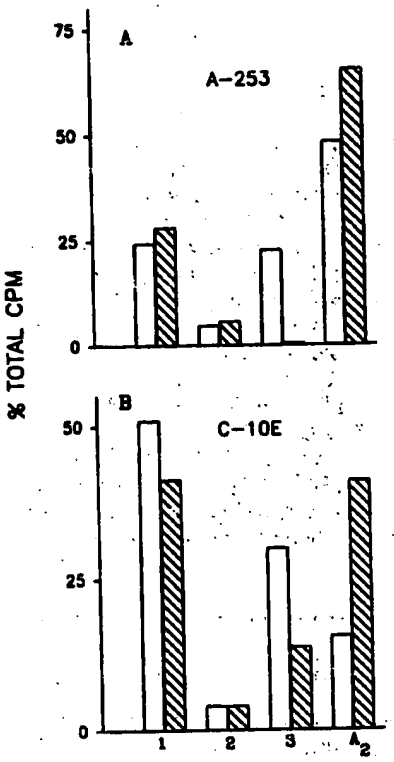


Fig. 5. Effect of E-64 pretreatment on the metabolism of [$^3$H]BLM $A_2$ in A-253 and C-10E cells. The amount of radioactivity in each peak (from Fig. 3) is expressed as a percentage of the total radioactivity. Peak 1 represents solvent front (fractions 2–5), peak 2 represents minor metabolite (fractions 9–11) and peak 3 represents the major metabolite (fractions 36–45). $A_2$ represents BLM $A_2$ (fractions 46–58). (A) Metabolism of [$^3$H]BLM $A_2$ after a 4-hr incubation with A-253 cells in the absence (open bars) or presence (hatched bars) of 2 mM E-64. The total radioactivity applied was 2063–2760 dpm. (B) Metabolism of [$^3$H]BLM $A_2$ after a 4-hr incubation with C-10E cells in the absence (open bars) or presence (hatched bars) of 2 mM E-64. Total radioactivity applied in these samples was 3418–4953 dpm.

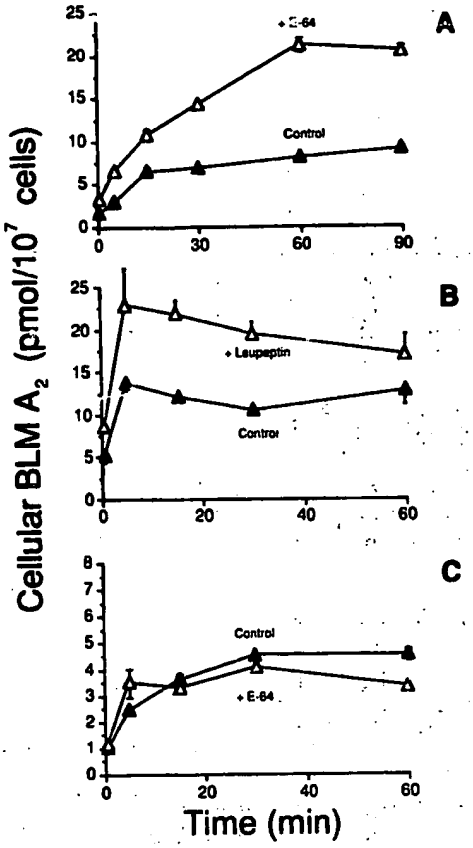


Fig. 6. (A) Enhancement of cellular association of [$^3$H]BLM $A_2$ in the presence of 2 mM E-64. Control flasks contained subconfluent A-253 cells grown with McCoy's modified medium. Experimental flasks contained the same medium to which 2 mM E-64 was added 3 days prior to assay. Cells were harvested, and the [$^3$H]BLM $A_2$ association was determined as described in Materials and Methods. (B) Enhancement of radioactive association of [$^3$H]BLM $A_2$ by leupeptin. A-253 cells were grown in McCoy's medium supplemented with 10% FBS in the presence or absence of 2 mM leupeptin for 3 days prior to harvesting. (C) Effect of E-64 on association of [$^3$H]BLM $A_2$ in C-10E cells. C-10E cells were grown in the presence or absence of 2 mM E-64 for the 3-day preincubation period. C-10E cell flasks contained no BLM for the preincubation period. Each point in the above figures is the average of six determinations; the SEM is included within the symbols unless noted by bars. Statistical significance was determined between E-64 pretreatment and no pretreatment samples at all time points using an unpaired Student's $t$-test ($P < 0.005$ for panel A and $P < 0.05$ for panel B).

The role of BLM metabolism in tumor cell resistance is controversial. Some investigators [6, 7, 23] have found that increased drug metabolism correlates with BLM resistance, whereas others [19, 24] have not. Recently, we demonstrated that BLM metabolism plays a major role in Burkitt's lymphoma *in vivo* [16]. The HPLC profile (Fig. 3) and histograms (Fig. 5) for BLM metabolism indicated that the BLM-resistant C-10E cell line did possess an increased capacity to metabolize BLM compared to the sensitive (A-253) cell line. Incubation with [$^3$H]BLM $A_2$ for 4 hr was required for this difference to be detected and the major metabolite (fractions 36–45) for the C-10E cell line did not appear to be the known metabolite produced by BH, dBLM $A_2$, which eluted earlier (fractions 23–25). The identity of the component(s) within this peak area is unknown but its formation is clearly cysteine proteinase dependent (see below).

We have also found that the resistant (C-10E) cell line accumulated 2- to 3-fold less BLM than did the drug-sensitive (A-253) cell line (Fig. 2). Although change in cellular drug association has been hypothesized as a means of BLM resistance [23–25], the C-10 [19] and C-10E cell lines are the first in which this has been demonstrated. We measured binding at 4° to differentiate between cell surface bound and internalized drug and found cell surface binding was also lower in resistant cells (Fig. 2C); the diminution in cell binding was approximately the same as the decrease in cellular drug association (2-

to 3-fold). Although the mode by which BLM enters cells is not known, cell surface binding has been suggested by previous microscopic [25] and biochemical [26] data. A previous kinetic study of BLM uptake supported a carrier-mediated transport process with a roughly equal number of specific and non-specific binding sites [26]. We also found that a portion of BLM binding could be blocked with excess unlabeled BLM, consistent with the presence of both non-specific and specific drug-binding sites. In the resistant cell line we found no change in $K_a$ for BLM, but could account for the lower steady-state levels of BLM by a 43% decrease in $V_{max}$ for drug association (Fig. 2B, inset). This observation would be consistent with a lower density for acceptor sites for BLM in the resistant (C-10E) cell line. Thus, the C-10E cells have two phenotypic properties that could produce resistance to BLM; we do not believe, however, that these two differences are related because the C-10E cells were derived from cells (C-10), which exhibited only decreased BLM $A_2$ association [19]. Continued selection pressure with BLM over 2 years has apparently resulted in the expression of a second mechanism of cellular resistance, increased drug metabolism, in the C-10E cell line.

The cysteine proteinase inhibitor, E-64, has been shown to inhibit BH *in vitro* [10, 27], and to potentiate the cytotoxicity of peplomycin against Chinese hamster lung cells in culture [17] and Ehrlich ascites-bearing mice *in vivo* [18]. Using isobologram analyses to evaluate drug interactions, we report here for the first time true pharmacological synergism between BLM and E-64 in both resistant and sensitive human tumor cell lines (Fig. 4). Nishimura *et al.* [17] suggested that potentiation of peplomycin cytotoxicity by E-64 is due to inhibition of BH; these investigators, however, found no significant change in total cellular content of drug (parent drug plus metabolites). The presence of several metabolites (fractions 9–11, 36–45) and the inhibition of the formation of one of these peaks (fractions 36–45) by treatment with E-64 (Figs. 3 and 5) could signal the existence of another cysteine proteinase capable of metabolizing the parent molecule or could indicate further metabolism of dBLM $A_2$. We are currently investigating the chemical nature and biological activity of these BLM metabolites.

In addition to effects on drug metabolism, E-64 and leupeptin were capable of increasing BLM $A_2$ cellular association. A-253 cells responded to either E-64 or leupeptin (Fig. 6, A and B) with a substantial increase in cellular BLM association. Surprisingly, the resistant (C-10E) cell line did not (Fig. 6C). This cannot be explained by a differential sensitivity to E-64 since the $IC_{50}$ values for both cell types were similar (5–7 mM). Thus, two separate cellular mechanisms: (1) inhibition of metabolism and (2) enhancement of cellular drug association may account for the synergism seen between cysteine proteinase inhibitors and BLM.

*Acknowledgements*—The authors wish to thank Ms. Leslie Najjar for her valuable assistance in the preparation of the figures. We also thank I. D. Braun, Beth Reffner and Celeste Reese for their technical advice and assistance. This investigation was supported by American Cancer Society Grants CH-316 (J.S.L.) and JFRA-248 (S.M.S.) and NIH Grants CA-48905 (S.M.S.) and CA-43917 (J.S.L.). G.M. was supported by NIH Fellowship IF32-CA-08880-01, and J.P.J. was supported by NIH Fellowship IF32-CA-08967-01.

## REFERENCES

1. Umezawa H, Recent progress in bleomycin studies. In: *Anticancer Agents Based upon Natural Product Models* (Eds. Cassady JM and Douros JD), pp. 147–166. Academic Press, New York, 1980.
2. Lazo JS and Sebti SM, Malignant cell resistance to bleomycin-group antibiotics. In: *Anticancer Drug Models* (Ed. Kessel D), pp. 267–279. CRC Press, Boca Raton, FL, 1989.
3. Carter SK, Bleomycin: More than a decade later. In: *Bleomycin Chemotherapy* (Eds. Sikic BI, Rozencweig M and Carter SK), pp. 3–4. Academic Press, Orlando, FL, 1985.
4. Young RC, Drug resistance: The clinical problem. In: *Drug Resistance in Cancer Therapy* (Ed. Ozols RF), pp. 1–3. Kluwer Academic Publishers, Norwell, MA, 1989.
5. Ozawa S, Suzuki H, Nishimura T and Tanaka N, Cellular uptake and efflux of peplomycin in sensitive and bleomycin-resistant subline of mouse lymphoblastoma L5178Y cells. *J Antibiot (Tokyo)* **41**: 395–397, 1988.
6. Miyaki M, Ono T, Hori S and Umezawa H, Binding of bleomycin to DNA in bleomycin-sensitive and bleomycin-resistant rat ascites hepatoma cells. *Cancer Res* **35**: 2015–2019, 1975.
7. Akiyama S-I, Ikezaki K, Kuramochi H, Takahashi K and Kuwano M, Bleomycin-resistant cells contain increased bleomycin hydrolase activities. *Biochem Biophys Res Commun* **101**: 55–60, 1981.
8. Sebti SM, DeLeon JC and Lazo JS, Purification, characterization and amino acid composition of rabbit pulmonary bleomycin hydrolase. *Biochemistry*. **26**: 4213–4219, 1987.
9. Sebti SM, DeLeon JC, Ma L-T, Hecht SM and Lazo JS, Substrate specificity of bleomycin hydrolase. *Biochem Pharmacol* **38**: 141–147, 1989.
10. Sebti SM, Mignano JE, Jani JP, Srimatkandada S and Lazo JS, Bleomycin hydrolase: Molecular cloning, sequencing and biochemical studies reveal membership in the cysteine proteinase family. *Biochemistry* **28**: 6544–6548, 1989.
11. Mascardo RN and Eilon G, The cysteine protease inhibitor, E-64, stimulates the polarization and locomotor responses of endothelial cells to wounding. *J Pharmacol Exp Ther* **244**: 361–367, 1988.
12. McCoy K, Gal S, Schwartz RH and Gottesman MM, An acid protease secreted by transformed cells interferes with antigen processing. *J Cell Biol* **106**: 1879–1884, 1988.
13. Gal S and Gottesman MM, The major excreted protein (MEP) of transformed mouse cells and cathepsin L have similar protease specificity. *Biochem Biophys Res Commun* **139**: 156–162, 1986.
14. Hanada K, Tamai M, Ohmura S, Sawada J, Seki T and Tanaka I, Structure and synthesis of E-64, a new thiol protease inhibitor. *Agric Biol Chem* **42**: 529–536, 1978.
15. Aoyagi T, Takeuchi T, Matsuzaki A, Kawamura K, Kondo S, Hamada M, Maeda K and Umezawa H, Leupeptins, new protease inhibitors from actinomycetes. *J Antibiot (Tokyo)* **22**: 283–286, 1969.
16. Sebti SM, Jani JP, Mistry JS, Gorelik E and Lazo JS, Metabolic inactivation: A mechanism of tumor resistance to bleomycin. *Cancer Res* **51**: 227–232, 1991.

17. Nishimura C, Nishimura T, Tanaka N, Yamaguchi H and Suzuki H, Inhibition of intracellular bleomycin hydrolase activity by E-64 leads to the potentiation of the cytotoxicity of peplomycin against Chinese hamster lung cells. *Jpn J Cancer Res* 80: 65–68, 1989.
18. Nishimura C, Nishimura T, Tanaka N and Suzuki H, Potentiation of the cytotoxicity of peplomycin against Ehrlich ascites carcinoma by bleomycin hydrolase inhibitors. *J Antibiot (Tokyo)* 40: 1794–1795, 1987.
19. Lazo JS, Braun ID, Larbee DC, Schisselbauer JC, Meandzija B, Newman RA and Kennedy KA, Characteristics of bleomycin-resistant phenotypes of human cell sublines and circumvention of bleomycin resistance by liblomycin. *Cancer Res* 49: 185–190, 1989.
20. Lazo JS and Humphreys CJ, Lack of metabolism as the biochemical basis of bleomycin-induced pulmonary toxicity. *Proc Natl Acad Sci USA* 80: 3064–3068, 1983.
21. Chou TC and Talalay P, Analysis of combined drug effects: A new look at a very old problem. *Trends Pharmacol Sci* 4: 450–454, 1983.
22. Zuckerman JE, Raffin TA, Brown JM, Newman RA, Etiz BB and Sikic BI, *In vitro* selection and characterization of a bleomycin-resistant subline of B16 melanoma. *Cancer Res*, 46: 1748–1753, 1986.
23. Suzuki H, Nishimura T and Tanaka N, Drug sensitivity and some characteristics of a bleomycin-resistant subline of mouse lymphoblastoma L5178Y cells. *J Antibiot (Tokyo)* 34: 1210–1212, 1981.
24. Lazo JS, Boland CJ and Schwartz PE, Bleomycin hydrolase activity and cytotoxicity in human tumors. *Cancer Res* 42: 4026–4031, 1982.
25. Fujimoto J, Radioautographic studies on the intracellular distribution of bleomycin-$^{14}C$ in mouse tumor cells. *Cancer Res* 34: 2969–2974, 1974.
26. Lyman S, Ujjani B, Renner K, Antholine W, Petering DH, Whetstone JW and Knight JM, Properties of the initial reaction of bleomycin and several of its metal complexes with Ehrlich cells. *Cancer Res* 46: 4472–4478, 1986.
27. Nishimura C, Suzuki H, Tanaka N and Yamaguchi H, Bleomycin hydrolase is a unique thiol aminopeptidase. *Biochem Biophys Res Commun* 163: 788–796, 1989.

This Page is inserted by IFW Indexing and Scanning Operations and is not part of the Official Record

# BEST AVAILABLE IMAGES

Defective images within this document are accurate representations of the original documents submitted by the applicant.

Defects in the images include but are not limited to the items checked:

- ☑ BLACK BORDERS
- ☐ IMAGE CUT OFF AT TOP, BOTTOM OR SIDES
- ☐ FADED TEXT OR DRAWING
- ☑ BLURED OR ILLEGIBLE TEXT OR DRAWING
- ☐ SKEWED/SLANTED IMAGES
- ☐ COLORED OR BLACK AND WHITE PHOTOGRAPHS
- ☐ GRAY SCALE DOCUMENTS
- ☑ LINES OR MARKS ON ORIGINAL DOCUMENT
- ☑ REPERENCE(S) OR EXHIBIT(S) SUBMITTED ARE POOR QUALITY
- ☐ OTHER: _____

**IMAGES ARE BEST AVAILABLE COPY.**
**As rescanning documents *will not* correct images problems checked, please do not report the problems to the IFW Image Problem Mailbox**